

Time averages and their statistical variation for the Ornstein-Uhlenbeck process: Role of initial particle distributions and relaxation to stationarity

Andrey G. Cherstvy,^{1,*} Samudrajit Thapa,¹ Yousof Mardoukhi,¹ Aleksei V. Chechkin,^{1,2} and Ralf Metzler^{1,†}

¹*Institute for Physics & Astronomy, University of Potsdam, 14476 Potsdam-Golm, Germany*

²*Institute for Theoretical Physics, Kharkov Institute of Physics and Technology, 61108 Kharkov, Ukraine*



(Received 25 April 2018; revised manuscript received 30 July 2018; published 28 August 2018)

How ergodic is diffusion under harmonic confinements? How strongly do ensemble- and time-averaged displacements differ for a thermally-agitated particle performing confined motion for different initial conditions? We here study these questions for the generic Ornstein-Uhlenbeck (OU) process and derive the analytical expressions for the second and fourth moment. These quantifiers are particularly relevant for the increasing number of single-particle tracking experiments using optical traps. For a fixed starting position, we discuss the definitions underlying the ensemble averages. We also quantify effects of equilibrium and nonequilibrium initial particle distributions onto the relaxation properties and emerging nonequivalence of the ensemble- and time-averaged displacements (even in the limit of long trajectories). We derive analytical expressions for the ergodicity breaking parameter quantifying the amplitude scatter of individual time-averaged trajectories, both for equilibrium and out-of-equilibrium initial particle positions, in the entire range of lag times. Our analytical predictions are in excellent agreement with results of computer simulations of the Langevin equation in a parabolic potential. We also examine the validity of the Einstein relation for the ensemble- and time-averaged moments of the OU-particle. Some physical systems, in which the relaxation and nonergodic features we unveiled may be observable, are discussed.

DOI: [10.1103/PhysRevE.98.022134](https://doi.org/10.1103/PhysRevE.98.022134)

I. INTRODUCTION

A. Ornstein-Uhlenbeck process

The paradigmatic model by Ornstein and Uhlenbeck originally published in 1930, see Refs. [1–8] (hereafter, the OU process), describes the diffusive Brownian motion (BM) of thermally-agitated particles [9–12] confined by an external parabolic potential, exerting a Hookean restoring force. Applications of this fundamental harmonic-oscillator model for physical, chemical, and biological problems are truly ubiquitous and range “from quarks to cosmology” [8]. Some important applications include financial economics [13–17], transition rates of chemical reactions [18], optically trapped objects and cells [19–22], ecology and adaptive evolution models [23], theoretical neuroscience [24,25], stochastic resonance (for bistable systems) [24,26], to mention a few. The stationarity of the OU process makes it an adequate candidate to describe and quantify deviations from steady-state behavior induced by thermal fluctuations.

The problems of escape and first-hitting time for harmonically-trapped particles were considered in Refs. [27–30]. Barrier-crossing Kramers-type problems for a thermally-activated escape [18,31] of trapped particles were also examined in double-well optical traps [32,33] and for fractional Gaussian noise [34]. Time-changed [35], fractional [36,37], and generalized OU processes in the presence of Lévy-stable noise [38–40] were studied as well. Time-averaged displacements and their statistical uncertainty for massive and massless

particles confined in an harmonic potential, also in the presence of dissipative/friction memory kernels, were considered in Ref. [41]. The dynamics of a quantum harmonic oscillator [42], a relativistic OU process [43,44] (see also Ref. [45]), and time- and space-fractional OU process [46–48] were investigated. A harmonic oscillator driven by colored noise [24,25] and effects of relaxation from nonequilibrium conditions [39] were examined; see Fig. 1.

Some models of harmonic oscillators with stochastic frequency, random noise and damping [8,49–51] were proposed (for ensemble averages). This temporal stochasticity of the model parameters is reminiscent of the “diffusing diffusivity” concept introduced recently [52–55]. The analog of fluctuating diffusion coefficients for BM [56] is the concept of stochastic volatility in financial economics and option-pricing models [13,57–61] described by Black-Scholes-Merton as geometric BM [62,63]. The concept of stochastic volatility is the standard tool for stochastic models of stock-price variations [14,15,64].

B. Time averaging and weak ergodicity breaking

The concepts of time averaging and nonergodicity were introduced for a number of diffusion processes, both normal and anomalous [65–67]. These quantifiers were computed for canonical BM [68–70], free and confined fractional BM, fractional Langevin equation motion [68,71–73], for free, confined, and aging continuous-time random walks [65,73–77], heterogeneous diffusion processes [78–81], scaled BM [81–85], ultraslow Sinai-like diffusion [83], for dynamics in disordered systems [86,87], random walks with memory [88], and Lévy walks [89].

In the standard Boltzmann-Khinchin sense, weak ergodicity breaking [90,91] signifies the nonequivalence of the

*a.cherstvy@gmail.com

†rmetzler@uni-potsdam.de

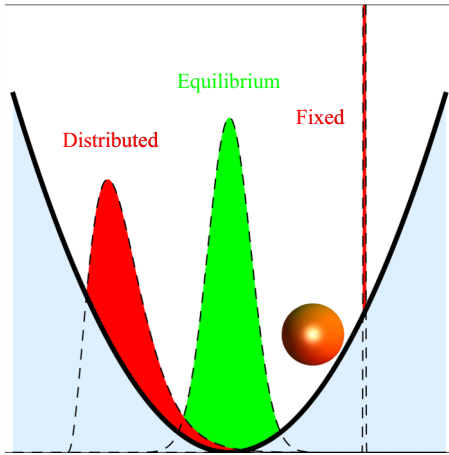


FIG. 1. Schematic of different initial particle distributions in a parabolic potential, as examined in the text for both equilibrium and nonequilibrium (fixed and distributed) cases.

ensemble- and time-averaged mean-squared displacements (MSDs) of a physical process in the long-time limit. In contrast, for strong ergodicity breaking, some regions of the phase space remain inaccessible on the timescale of particle diffusion, which might depend on initial conditions of the system [67,91–93]. The phenomena of weak ergodicity breaking for long trajectories and anomalous diffusion [66,67,94–98] were repeatedly detected in cellular biological systems, inter alia, for tracer diffusion in the cytoplasm of living cells, lipid, and protein motion on biomembranes, internal dynamics of proteins, diffusion of chromosomal loci, motion of proteins, viruses, and RNAs inside cells (see recent reviews [66,67]). In particular, the behavior of ensemble- and time-averaged MSDs as well as the ergodicity breaking parameter (denoted EB) for fractional BM and generalized Langevin equation motion under power-law memory kernel—confined both by infinite square wells [71] and by a parabolic potential [72]—were investigated. Despite the asymptotically ergodic nature of these processes, transient nonergodic behavior was shown to occur [68,99].

C. Trapping and tracking of tracer particles

A number of single-particle manipulation and tracking experiments [99–112] performed, e.g., in living cells utilize localization properties of dielectric particles in optical traps [21,22,109,113,114,117]. Such optical “tweezers” create a *parabolic potential* for tracer motion: the restoring force is linear in particle displacement from the center of the trap (allowed displacements are often $\lesssim 400$ nm [22]). Optical tweezers enable secure trapping in all three spatial dimensions and high-precision manipulation of micro- and nanosized objects, also inside biological cells [22,103]. Provided the laser energies and densities are significantly low and the exposure times are short enough [103], trapping of particles in complex, dynamic, and heterogeneous environments of the cell cytoplasm by infrared-laser optical tweezers is rather noninvasive [115]. Some calibration issues [103,116,118,119] and trap-stiffness estimations [120] for this setup were reported (also for a time-dependent trap stiffness [121]). Typically, such single-particle tracking experiments record fairly long but not

so many trajectories, which are later evaluated in terms of time averages rather than ensemble averages. This prompts a detailed study of relevant physical observables and their ergodic behavior in an harmonic potential.

The experimental trap-stiffness (spring-constant) values used for biological cells are $k \sim 0.01 \dots 1$ pN/nm [22,103] (often, however, in a lower part of this range, see $k \sim 0.05$ pN/nm in Ref. [99]). The spatial resolution of the optical trap apparatus is $0.1 \dots 2$ nm [22] and particle sizes can vary from several tens of nm to several microns (see Refs. [115,116] for the trap characteristics used in living cells). Numerical simulations of optically trapped particles with inertia [33] and theoretical investigations of massive particles in harmonic traps [106] were conducted. Here, we also mention single-molecule setups for monitoring tethered particle motion [22,122], with often parabolic potentials acting, e.g., on a magnetic bead tethered to a DNA molecule due to entropic elasticity of the DNA [123].

We focus below on deviations of the time-averaged and ergodic characteristics of the OU process. We find that—particular for nonequilibrium initial particle conditions in an harmonic potential relevant in single-particle systems—the discrepancy of the ensemble- and time-averaged MSDs may turn out to be very pronounced. Note that, in addition to the standard particle-displacement characteristics, additional statistical methods and classifiers exist for the analysis of single-particle trajectories [124–128].

D. Structure of the paper

The paper is organized as follows. We present the main analytical results for the ensemble- and time-averaged MSDs of the OU process in Sec. II A, both for equilibrium and nonequilibrium initial particle conditions. In Sec. II A 3 we discuss possible alternative definitions of particle-displacement characteristics for diffusion in external potentials. In Sec. II B we examine the behavior of the ergodicity breaking parameter for confined OU motion, EB_{OU} . To the best of our knowledge, the exact expression for EB_{OU} for arbitrary initial particle positions is not known. The analytical evaluation of EB for a thermally-driven particle in an harmonic potential—useful for the examination of physical data—is the main mathematical challenge of this study.

The behavior of displacements and EB parameter are rationalized for equilibrium and nonequilibrium (fixed and distributed) initial particle conditions. These choices reflect initial preparations of the system, before the start of the measurement. The first choice is to start with an initial thermal equilibrium, while the second scenario is a δ -function-like initial position. The third, and often most complicated, scenario involves an arbitrary distribution of starting positions, $P(x_0)$; see Fig. 1. For the latter, the second moments of displacements and EB become functions of the moments of $P(x_0)$, denoted as $\langle x_0^2 \rangle$ and $\langle x_0^4 \rangle$. We note that nonthermal initial conditions are a fairly standard situation in single-particle experiments, e.g., when a tracer is initially captured by the tweezers potential (when the trap is located close to the particle). In Sec. II C we present the linear-response relations for the ensemble- and time-averaged characteristics of the OU process. The conclusions are presented in Sec. III A and possible applications of

our findings are outlined in Sec. III B. Technical details of the derivations are given in Appendix A.

II. MAIN RESULTS

A. Ensemble- and time-averaged displacements

As most prominent quantifiers of diffusive processes, we first compute the ensemble- and time-averaged MSDs of a particle confined by the harmonic potential

$$U(x) = kx^2/2 \equiv \lambda x^2/(2\mu). \quad (1)$$

Here, the particle mobility is μ and the spring constant of the potential is $k = \lambda/\mu$. Below, we perform the analysis (for simplicity, in one dimension only, higher dimensions can be viewed component-wise) for arbitrary initial positions, $x(t=0) = x_0$, both fixed and distributed. We start with the *overdamped* Langevin equation for diffusion of a pointlike particle *without inertia* effects,

$$dx(t)/dt + \lambda x = \sigma \xi(t), \quad (2)$$

driven by the white (δ -correlated) noise

$$\langle \xi(t)\xi(t') \rangle = \delta(t - t'), \quad (3)$$

with zero mean, $\langle \xi(t) \rangle = 0$. Inertial effects can typically be neglected for long-time diffusion of standard tracer particles. The diffusion coefficient is connected to the noise intensity as

$$D = \sigma^2/2, \quad (4)$$

and we suppose that the Stokes-Einstein-Smoluchowski relation holds,

$$D = \mu k_B \mathcal{T}, \quad (5)$$

where $k_B \mathcal{T}$ is the thermal energy. The general solution of the stochastic differential Eq. (2) is

$$x(t) = x_0 e^{-\lambda t} + \int_0^t dt' \sigma \xi(t') e^{-\lambda(t-t')}, \quad (6)$$

where $1/\lambda$ is the relaxation time. Performing averaging over *both* noise realizations $\xi(t)$ and initial positions x_0 (denoted by the angular brackets) the solution for the second moment of displacement with respect to initial position (the standard MSD; see also Sec. II A 3) becomes

$$\langle (x(t) - x_0)^2 \rangle = \langle x_0^2 \rangle (1 - e^{-\lambda t})^2 + \frac{\sigma^2}{2\lambda} (1 - e^{-2\lambda t}). \quad (7)$$

Constructing from the Langevin Eq. (2) the time-independent Fokker-Planck equation for the equilibrium (subscript “eq”) probability density of particle positions (see, e.g., Refs. [1,5–7]),

$$D \frac{d^2 P_{\text{eq}}(x)}{dx^2} = \frac{d}{dx} \left[-\mu \frac{dU(x)}{dx} P_{\text{eq}}(x) \right], \quad (8)$$

we find its solution as the Boltzmann distribution,

$$P_{\text{eq}}(x) = \sqrt{\frac{\lambda}{\pi \sigma^2}} \exp\left(-\frac{\lambda x^2}{\sigma^2}\right) = \sqrt{\frac{\mu k}{2\pi D}} \exp\left[-\frac{\mu U(x)}{D}\right]. \quad (9)$$

Using this steady-state displacement distribution, the *thermal value* for the particle displacement at equilibrium is

$$\langle x_{\text{eq}}^2 \rangle = \int_{-\infty}^{+\infty} x^2 P_{\text{eq}}(x) dx = \frac{\sigma^2}{2\lambda} = \frac{\mu k_B \mathcal{T}}{\lambda} = \frac{k_B \mathcal{T}}{k}, \quad (10)$$

due to energy equipartitioning [22]. This allows us to rewrite Eq. (7) in the form

$$\begin{aligned} \langle (x(\Delta) - x_0)^2 \rangle &= 2\langle x_{\text{eq}}^2 \rangle (1 - e^{-\lambda \Delta}) \\ &+ (\langle x_0^2 \rangle - \langle x_{\text{eq}}^2 \rangle) (1 - e^{-\lambda \Delta})^2. \end{aligned} \quad (11)$$

Using the general solution (6) the pair correlation function for positions of the particle performing the OU process is

$$\langle x(t')x(t'') \rangle = (\langle x_0^2 \rangle - \langle x_{\text{eq}}^2 \rangle) e^{-\lambda(t'+t'')} + \langle x_{\text{eq}}^2 \rangle e^{-\lambda|t'-t''|}. \quad (12)$$

For the time-averaged MSD—defined for a stochastic process $x(t)$ via [65–67]

$$\overline{\delta^2(\Delta)} = \frac{1}{T - \Delta} \int_0^{T-\Delta} [x(t + \Delta) - x(t)]^2 dt, \quad (13)$$

and denoted below by the overline—the integration of Eq. (13) using Eq. (12) yields, after averaging over an ensemble of N trajectories,

$$\overline{\delta^2(\Delta)} = N^{-1} \sum_{i=1}^N \overline{\delta_i^2(\Delta)}, \quad (14)$$

that

$$\begin{aligned} \overline{\delta^2(\Delta)} &= 2\langle x_{\text{eq}}^2 \rangle (1 - e^{-\lambda \Delta}) \\ &+ (\langle x_0^2 \rangle - \langle x_{\text{eq}}^2 \rangle) (1 - e^{-\lambda \Delta})^2 \frac{1 - e^{-2\lambda(T-\Delta)}}{2\lambda(T-\Delta)}. \end{aligned} \quad (15)$$

Here, the lag time is Δ and T denotes the length of the trajectory (observation time).

For $x_0 = 0$ the expressions for the time-averaged MSD for standard and fractional BMs were derived in Eqs. (3) and (13) of Ref. [72]. We refer the reader also to Ref. [41] for derivations of the time-averaged MSD of harmonically-confined particles (see Sec. III A in Ref. [41]), the fourth-order correlation function of particle positions, and the statistical uncertainty of time-averaged MSD realizations (see Appendix A of Ref. [41]). The statistical uncertainty mentioned here is the square root of the EB parameter computed below.

1. Equilibrium initial conditions

When the initial particle positions x_0 are chosen to satisfy the *equilibrium distribution* (9), one gets

$$\langle x_0^2 \rangle = \langle x_{\text{eq}}^2 \rangle. \quad (16)$$

Therefore, the second terms in Eqs. (11) and (15) disappear and the pair correlator (12) becomes exponential,

$$\langle x(t')x(t'') \rangle_{\text{eq}} = \langle x_{\text{eq}}^2 \rangle e^{-\lambda|t'-t''|}. \quad (17)$$

In this scenario, the particles are equilibrated in the potential before starting their motion and the ensemble- and time-averaged MSDs *coincide* in the entire range of lag times (diffusion is fully ergodic, see Sec. II B for details).

The behavior of the MSD is illustrated in Figs. 2(a) and 2(b). For equilibrated starting conditions (the green curves in the

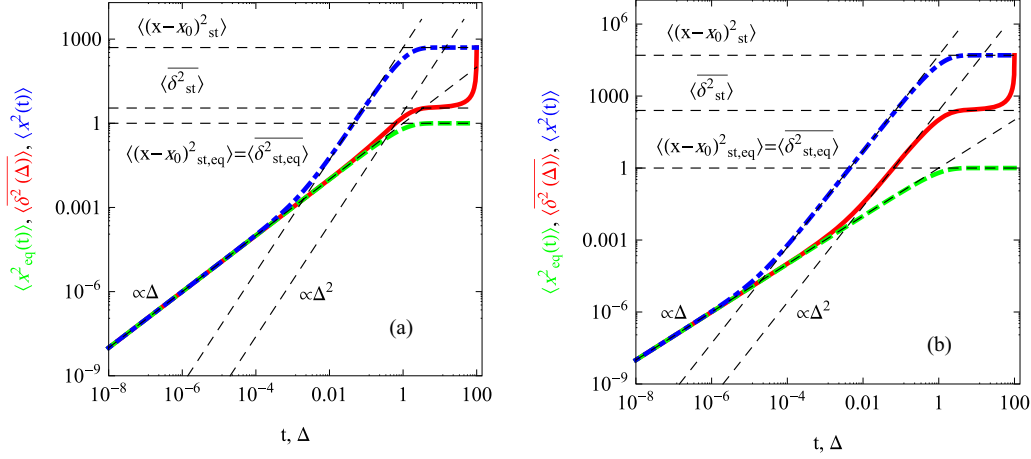


FIG. 2. Ensemble- and time-averaged MSDs for the OU process with equilibrium and nonequilibrium initial particle positions x_0 , plotted versus (lag) time. The linear and ballistic asymptotes of Eqs. (21) and (22) and the plateau values of Eqs. (19), (23), and (24) are the dashed lines. Parameters: $T = 10^2$, $\lambda = 1$, $\sigma = 1$, $\langle x_0^2 \rangle = 10^3 \langle x_{\text{eq}}^2 \rangle$ (panel a) and $\langle x_0^2 \rangle = 10^5 \langle x_{\text{eq}}^2 \rangle$ (panel b).

plot) at short times the MSD of Eq. (7) and time-averaged MSD of Eq. (15) grow nearly unperturbed as $\sigma^2 t \approx 2Dt$. After a characteristic timescale,

$$t \gg t^* \sim 1/\lambda, \quad (18)$$

the MSD and time-averaged MSD start approaching the stationary (subscript “st” below) plateau value,

$$\langle (x - x_0)_{\text{st,eq}}^2 \rangle = \langle \delta_{\text{st,eq}}^2 \rangle = \sigma^2/\lambda = 2\langle x_{\text{eq}}^2 \rangle. \quad (19)$$

2. Nonequilibrium initial conditions

The MSD and time-averaged MSD develop very differently and *nonergodically* if initial positions x_0 are not equilibrated, as illustrated in Figs. 2(a) and 2(b). In particular, if we start strongly out-of-equilibrium, where

$$\langle x_0^2 \rangle \gg \langle x_{\text{eq}}^2 \rangle, \quad (20)$$

both ensemble- and time-averaged MSDs after the unconfined initial *linear* growth can have a region of *ballistic* diffusion. Specifically, in this limit the Taylor expansion of Eqs. (11) and (15) at short lag times gives, respectively,

$$\langle (x(\Delta) - x_0)^2 \rangle \approx \sigma^2 \Delta + \lambda^2 \langle x_0^2 \rangle \Delta^2 \quad (21)$$

and

$$\langle \overline{\delta^2(\Delta)} \rangle \approx \sigma^2 \Delta + \lambda \langle x_0^2 \rangle \Delta^2 / (2T). \quad (22)$$

Here, we consider long traces $\lambda T \gg 1$ and strongly nonequilibrium starting positions, Eq. (20). From Eqs. (21) and (22) we find that the ballistic region for the MSD starts *much earlier* than that for the time-averaged MSD. The latter becomes ballistic at the lag time at which the second term in Eq. (22) starts to dominate over the short-time Fickian motion. This ballistic regime is pronounced for larger $\langle x_0^2 \rangle$ values, as expected: it describes rapid relaxation to the bottom of the potential well (1).

For starting positions *close to* the equilibrium Eq. (10), the ballistic regime can almost disappear in the time-averaged MSD, while the ensemble-averaged MSD still exhibits roughly ballistic growth over a substantial time range. The evolution

of the ensemble- and time-averaged MSDs for nonequilibrium starting conditions is illustrated in Figs. 2(a) and 2(b) by the blue and red curves, respectively. At intermediate times, these quantities relax quite differently: both their magnitudes and scaling exponents can be substantially different. This may have severe implications for different averaging protocols employed in single-particle tracking experiments monitoring tracers in confining potentials; see Sec. III.

We also observe that after a region of ballistic MSD growth—if the trajectories are long enough—a *stationary* regime is reached. When the conditions $\lambda \Delta \gg 1$ and $\Delta \ll T$ are satisfied, the steady-state plateaus for the ensemble- and time-averaged MSDs follow from Eqs. (11) and (15) as

$$\langle (x - x_0)_{\text{st}}^2 \rangle \approx \langle x_0^2 \rangle + \langle x_{\text{eq}}^2 \rangle \quad (23)$$

and

$$\langle \overline{\delta_{\text{st}}^2} \rangle \approx 2\langle x_{\text{eq}}^2 \rangle + \frac{\langle x_0^2 \rangle - \langle x_{\text{eq}}^2 \rangle}{2\lambda T}. \quad (24)$$

The two averages are equal only for equilibrium starting conditions, Eq. (19). As the stationary time-averaged MSD in Eq. (24) depends on the trace length T , the plateaus of the ensemble- and time-averaged MSDs can differ strongly for nonequilibrium starting conditions; see Fig. 2. Finally, at the very end of particle trajectories, the ensemble- and time-averaged MSDs coincide, as they should [67]. At the very last point $\Delta = T$ both averages reach the plateau Eq. (23); see Fig. 2. Interestingly, the time-averaged MSD reveals a rapid increase at $\Delta \rightarrow T$ that becomes sharper for longer traces (not shown).

In Fig. 3 we illustrate the reproducibility of individual realizations δ_i^2 for different trace lengths. As expected, the spread of trajectories reduces with the trace length, reflecting the reciprocal dependence $\text{EB}(T) \sim 1/T$, as we observe for short lag times [see Eq. (26) and the discussion below]. The spread of time-averaged MSD magnitudes is minimal at short lag times Δ . Also similar to BM, the spread of $\delta_i^2(\Delta)$ grows with the lag time, reaching maximal irreproducibility at $\Delta \rightarrow T$, due to the naturally worsening statistics [41,66,67].

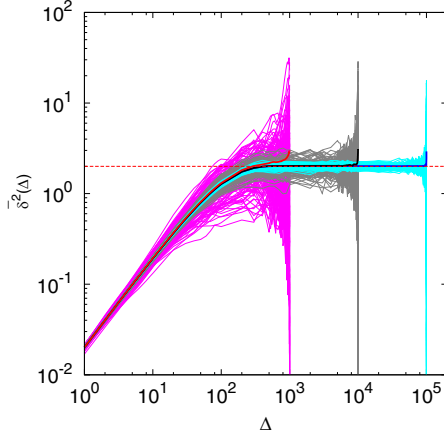


FIG. 3. Trajectory-to-trajectory variations of time-averaged MSDs for the OU process, obtained for traces of $T = \{10^3, 10^4, 10^5\}$ steps from computer simulations of Eq. (2) with integration time step $dt = 0.01$. The respective ensemble averages of Eq. (14) are the thick curves for each T . Initial positions are normally distributed, with $P_{\text{eq}}(x_0) = \exp(-x_0^2/2)/\sqrt{2\pi}$ (with $\lambda = 1$ and $\sigma = \sqrt{2}$). The asymptote (24) is the dashed line. We show $N = 10^2$ traces for each length T to demonstrate a *decreasing* spread of time-averaged MSDs for longer traces. Also note that the statistics is best at $\Delta \ll T$, as expected.

3. Definitions: Standard MSD versus displacement increments average

Note that for the *nonshifted* second moment, $\langle x^2(t) \rangle$, the plateau value is only *half* as high as compared to Eq. (19), that is $\langle x^2(t \rightarrow \infty)_{\text{st,eq}} \rangle \rightarrow \sigma^2/(2\lambda)$. Therefore, in the steady-state a *spurious factor* of two emerges between the ensemble- and time-averaged displacements; see Refs. [41,72,80,104,106,129]. The definition of Eq. (7) “cures” this apparent inconsistency and restores the equality of both averages in the long-time limit Eq. (19). We also refer the reader to the Discussion section in Ref. [72] for some alternative definitions of time averaging.

Moreover, for diffusion in *any* potential (including confining ones), the standard definition of the MSD involves a translationally noninvariant initial position x_0 that may lead to seemingly paradoxical results. One of them is, e.g., the factor of *two* difference between the stationary ensemble and time-averaged MSDs in Eq. (24). For nonstationary motion in a potential, such as the OU process, for *arbitrary* initial position a viable definition may involve increments along the trajectory $\langle (x(t + \Delta) - x(t))^2 \rangle$. In harmonic potentials this yields

$$\begin{aligned} \langle (x(t + \Delta) - x(t))^2 \rangle &= 2\langle x_{\text{eq}}^2 \rangle (1 - e^{-\lambda\Delta}) \\ &+ (\langle x_0^2 \rangle - \langle x_{\text{eq}}^2 \rangle) (1 - e^{-\lambda\Delta})^2 e^{-2\lambda t}, \end{aligned} \quad (25)$$

that after averaging over time t is evidently identical to $\overline{\delta^2(\Delta)}$ in Eq. (15). So, the increments of particle displacements in Eqs. (25) and (15) may be chosen for comparison particle diffusive characteristics in confining potentials. For the OU process, the definition (25) for the ensemble-averaged displacements yields results *identical* to the time-averaged MSD Eq. (15) and thus *ergodic* diffusion is realized at all

times, see also Ref. [33]. Practically, however, the definition of Eq. (25) is rarely being used.

We therefore aim at pointing the attention of the experimental community performing single-particle tracking in external potentials to this conceptual difference in the displacement definitions. The standard MSD in Eq. (11) involves the initial particle position and yields an inequality of the ensemble- and time-averaged MSDs. In contrast, the increment-based definition Eq. (25) gives rise to ergodic diffusion, as expected for the OU diffusion process. In what follows, we use the canonical definitions for the ensemble- and time-averaged MSDs, Eqs. (7) and (13), as well as the for EB Eq. (26), and we study the consequences.

B. Ergodicity-breaking parameter

A by-now well-established measure of nonergodicity of a stochastic process $x(t)$ is the ergodicity breaking parameter, EB. It quantifies the irreproducibility of individual time-averaged MSDs as a function of lag time Δ . The EB parameter is defined via the fourth moment of time-averaged particle displacements as [66–68,130]

$$\text{EB}(\Delta, T) = \left\langle \overline{\delta^2(\Delta, T)}^2 \right\rangle / \left\langle \overline{\delta^2(\Delta, T)} \right\rangle^2 - 1. \quad (26)$$

This parameter delivers statistically most reliable information for short lag times, $\Delta \ll T$, as the time-averaged MSD itself [67,79,84]. We first consider equilibrium distributions of initial positions of the OU particles. In this case, diffusion remains Gaussian and the fourth moment of the time-averaged displacements for solution of Eq. (6) can be computed using the Isserlis-Wick theorem for zero-mean processes. The derivation of $\left\langle \overline{\delta^2(\Delta)}^2 \right\rangle$ in Eq. (26) is based on splitting the four-point correlator into the sum of products of two-point correlators Eq. (12); see Appendix A. Below, we present analytical and computer simulation results for EB of the OU process, EB_{OU} . Note that for other-than-parabolic confinements the EB calculations can be harder (not considered here). For BM the probability distribution of time-averaged MSDs as well as its higher moments—skewness and kurtosis—were computed recently [69]; see also Refs. [41,70,131]. For other Gaussian (and slightly nonergodic) processes—such as scaled [83,84] and fractional [68,73] BMs—the EB parameter was also evaluated.

1. Equilibrium initial conditions

For the OU process we compute the EB parameter separately for $0 < \Delta < T/2$ and $T/2 < \Delta < T$, denoting the respective quantities $\text{EB}_{\text{OU}, <}$ and $\text{EB}_{\text{OU}, >}$. A similar procedure of interval division was employed for computing higher-order moments of free BM [69]. For the *equilibrium* initial particle positions (16) the EB parameter becomes (see Appendix A for derivations)

$$\begin{aligned} \text{EB}_{\text{OU,eq}, <}(\Delta, T) &= -1 + \frac{e^{-2\lambda T}}{[2(e^{\lambda\Delta} - 1)\lambda(\Delta - T)]^2} \\ &\times (e^{2\lambda\Delta} - 4e^{3\lambda\Delta} + 6e^{4\lambda\Delta} - 4e^{5\lambda\Delta} + e^{6\lambda\Delta} \\ &+ 4e^{2\lambda T} \{-1 + \lambda[-2\Delta(1 + \lambda\Delta) + T + \lambda T^2]\} \\ &+ 8e^{\lambda(\Delta+2T)} \{1 + \lambda[3\Delta + 2\Delta^2\lambda - T(2 + \lambda T)]\} \\ &+ 4e^{2\lambda(\Delta+T)} \{-1 + \lambda[\Delta^2\lambda - 2\Delta(2 + \lambda T) \\ &+ T(3 + \lambda T)]\}) \end{aligned} \quad (27)$$

and

$$\begin{aligned}
 \text{EB}_{\text{OU,eq},>}(\Delta, T) = & -1 + \frac{e^{-2\lambda(\Delta+T)}}{[2(e^{\lambda\Delta} - 1)\lambda(\Delta - T)]^2} \\
 & \times \{e^{4\lambda\Delta} - 4e^{5\lambda\Delta} + 4e^{6\lambda\Delta} + e^{4\lambda T} \\
 & + 2e^{2\lambda(\Delta+T)}(-1 + 2\Delta\lambda - 2\lambda T)(1 + 2\Delta\lambda - 2\lambda T) \\
 & - 4e^{3\lambda\Delta+2\lambda T}[-1 + 2\lambda(\Delta - T)(-1 + 2\lambda\Delta - 2\lambda T)] \\
 & + 4e^{2\lambda(2\Delta+T)}[-1 + \lambda(\Delta - T)(-2 + \lambda\Delta - \lambda T)]\}. \quad (28)
 \end{aligned}$$

These expressions for EB and its first derivative over lag time are continuous at $\Delta = T/2$, similar to Eqs. (32) and (33) below for free BM [69].

For short lag times, $\Delta/T \ll 1$, and toward the end of the trajectory, $(T - \Delta)/T \ll 1$, expansion of Eqs. (27) and (28) for conditions of weak confinement yields, respectively,

$$\text{EB}_{\text{OU,eq},<}(\Delta) \approx 4\Delta/(3T) - \lambda\Delta^2/(6T) \quad (29)$$

and

$$\text{EB}_{\text{OU,eq},>}(\Delta) \approx 2 - 4\lambda(T - \Delta)/3. \quad (30)$$

Here, the limit of long traces $\lambda T \gg 1$ was employed, similar to the condition used to obtain the MSD expansions given by Eqs. (21) and (22). The stationary value of EB follows from Eq. (27) in the limit $\lambda\Delta \gg 1$ and for measurement times much longer than the correlation time, $T \gg 1/\lambda$, namely,

$$\text{EB}_{\text{OU,eq,st}}(T) \approx 3/(\lambda T) \simeq 1/T. \quad (31)$$

This plateau value was predicted for the case of general Gaussian processes before, see Eq. (60) in Ref. [41], similarly to the limiting value of $\text{EB}=2$ in the limit $\Delta \rightarrow T$. Note, however, that neither general analytical formulas for the EB parameter were presented in Ref. [41], nor the effect of equilibrium versus nonequilibrium initial in positions was examined there, which is our main focus here. Therefore, for very long trajectories the EB parameter for the OU-particle approaches zero, indicating an intrinsic ergodicity of the process. This is true both at short lag times in Eq. (29) and in the stationary regime (31), featuring the same functional form $\text{EB}(T) \propto 1/T$ as BM [67,69], free and confined fractional BM [71,72], scaled BM [81,84], and (in some limits) heterogeneous diffusion processes [80,81]. The leading behavior in Eq. (31) involves two timescales, $1/\lambda$ and T .

For free BM the EB parameter (or reduced variance, κ_2/κ_1^2) was evaluated in Ref. [69] via the first two cumulant moments [6], κ_1 and κ_2 . For lag times in the domains $0 < \Delta < T/2$ and $T/2 < \Delta < T$ —denoted by subscripts “<” and “>” below—the expressions for EB are, respectively,

$$\text{EB}_{\text{BM},<}(\Delta) = \frac{\Delta(4 - 5\Delta/T)}{3T(1 - \Delta/T)^2} \quad (32)$$

and

$$\text{EB}_{\text{BM},>}(\Delta) = \frac{11(\Delta/T)^2 - 6(\Delta/T) + 1}{3(\Delta/T)^2}. \quad (33)$$

At short lag times, $\Delta/T \ll 1$, the canonical result for the linear growth of $\text{EB}(\Delta)$ follows from Eq. (32) as [41,67–69,73]

$$\text{EB}_{\text{BM}}(\Delta) \approx 4\Delta/(3T). \quad (34)$$

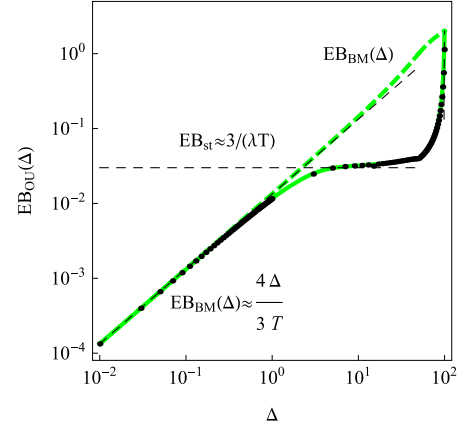


FIG. 4. Ergodicity breaking parameter for the OU process versus lag time, plotted for the parameters of Fig. 2 at equilibrium starting conditions, Eqs. (27) and (28). The results of numerical integration of the fourth moment in Eq. (A3) are the data points. The results for free BM, Eqs. (32) and (33), is the dashed green curve. The short-time asymptote of Eq. (34), the stationary plateau of Eq. (31), and the expansion of Eq. (30) at $\Delta \rightarrow T = 10^2$ are the dashed black lines.

In the end of the traces, the universal value $\text{EB} = 2$ is approached, with the expansion at $\Delta \rightarrow T$ (see also Ref. [41]),

$$\text{EB}_{\text{BM}}(\Delta) \approx 2 - 4(T - \Delta)/(3T). \quad (35)$$

Figure 4 presents the evolution of $\text{EB}(\Delta)$ as obtained from our analytical and numerical calculations. The green color in Figs. 4 and 5 reflects equilibrium starting conditions, as in Figs. 1 and 2. We observe that at short lag times the particles diffuse unperturbed, with EB growth similar to that of free BM, as expected. After a characteristic time $\Delta^* \sim 1/\lambda$, EB starts developing a stationary plateau. For longer trajectories the plateau region occupies a more substantial fraction of lag times; see Fig. 5. For short lag times and in the stationary regime $\text{EB}(T)$ in simulations scales as $1/T$, supporting theoretical Eqs. (29) and (31), see the plot and the inset in Fig. 5.

For long lag times, at $\Delta \rightarrow T$ a rather *rapid growth* of $\text{EB}(\Delta)$ takes place, from the stationary value given by Eq. (31) to the value $\text{EB} = 2$ at $\Delta = T$. This terminal EB value at $\Delta = T$ is the same for (free and confined) BM and fractional BM [69,71,72]. For longer trajectories the EB plateau of Eq. (31) decreases, and thus the approach to the limiting value $\text{EB} = 2$ at $\Delta \rightarrow T$ becomes sharper. Interestingly, the OU-particles diffuse “*more ergodically*” than Brownian particles, i.e., $\text{EB}_{\text{OU}}(\Delta) < \text{EB}_{\text{BM}}(\Delta)$ for the same Δ and T . For quasistationary diffusion (at intermediate lag times and long trajectories) EB_{OU} can be dramatically smaller than EB_{BM} ; see Fig. 5.

Our theoretical predictions are in excellent agreement with the results of stochastic simulations of Eq. (2) in the entire range of lag times. Figure 5 illustrates the variation of $\text{EB}(\Delta)$ for varying T for initial particle positions being at equilibrium, Eq. (9). Note that to capture the rapid EB increase from the plateau value at intermediate lag times to $\text{EB} = 2$ at $\Delta \rightarrow T$, a denser lag-time sampling was implemented.

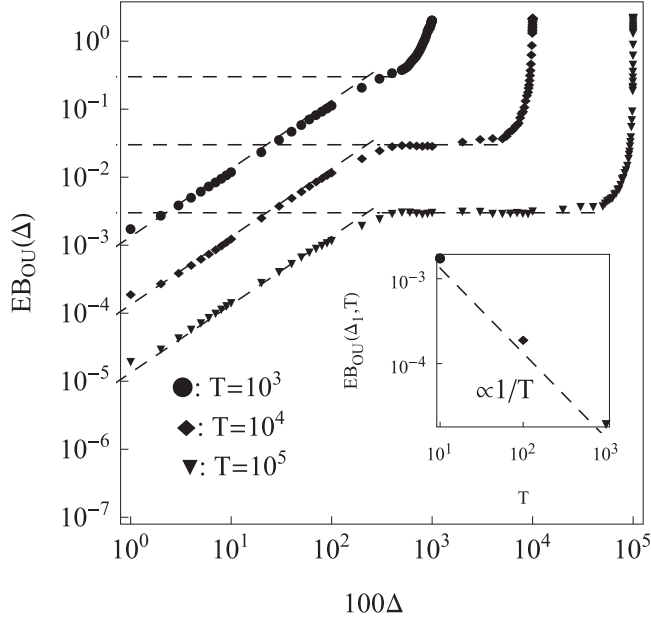


FIG. 5. Computer simulations results for the EB parameter of harmonically-confined particles with equilibrium initial conditions, plotted for the parameters of Fig. 3. The trajectory lengths are $T = \{10^1, 10^2, 10^3\}$ and the integration step is $\delta t = 0.01$ (mention the 10^2 -factor for the abscissa axis). Asymptotic behavior for free BM given by Eq. (34) and the plateaus of Eq. (31) are the dashed lines. Averaging over $N = 10^3$ traces was performed. The inset shows EB values at the minimal lag time $\Delta_1 = 0.01$ plotted versus the trace length T , together with the Brownian asymptote of Eq. (34).

2. Nonequilibrium initial conditions

For *arbitrary and nonequilibrium* initial particle conditions, the analytical derivation of EB is considerably harder; see Appendix B. The general analytical results for EB are provided in Eqs. (B4) and (B5). We start with a simpler case of *fixed and nondistributed* x_0 values; see Fig. 6. The analytically predicted initial linear growth of EB with the lag time as for free BM, Eq. (34), a sublinear growth of EB(Δ) at intermediate lag times, stationary EB values for even larger Δ values, Eq. (B12), and, finally, the behavior EB($\Delta \rightarrow T$) in the end of the trajectory, Eq. (B13), are all in quantitative agreement with the results of computer simulations. We find that for larger x_0 the EB plateau becomes smaller—compare the curves in Fig. 6 for different x_0 —as Eq. (B12) predicts. In contrast, for small x_0 values the results for EB are close to those for equilibrium starting positions, compare the data points and the green curve in Fig. 6. Note that in Fig. 6 *no ballistic* EB(Δ) growth at intermediate lag times is found. The reason is that for fixed starting positions $\langle x_0^4 \rangle = \langle x_0^2 \rangle^2$ and thus the terms quadratic in the lag time in Eq. (B6) give rise to a *reduction* of EB in this range of lag times.

EB behaves very differently for *strongly nonequilibrium* $P(x_0)$ distributions; see Fig. 7. We find that EB first grows linearly with the lag time, similarly as for BM, Eq. (34). At intermediate lag times, a region of a *quadratic growth* can emerge, as Eq. (B6) predicts. This faster-than-linear EB(Δ) growth is reminiscent of that for the ensemble and time-averaged MSDs in Sec. II A and Fig. 2. After the ballistic

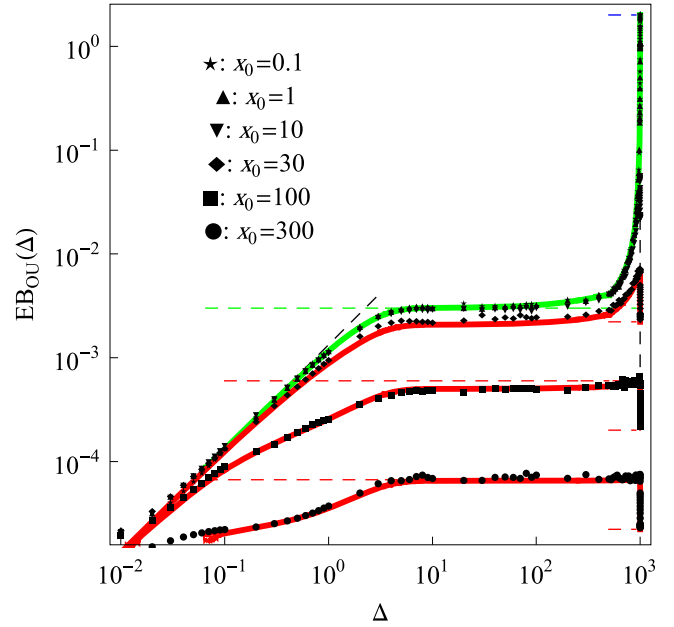


FIG. 6. Results for EB_{OU} from stochastic computer simulations at *varying* initial positions x_0 (given in the legend). The results of Fig. 5 for normally-distributed x_0 for $T = 10^3$ are shown as the full green curve. The full analytical results Eqs. (B4) and (B5) are the full solid curves. The red-green color scheme for the solid curves reflects equilibrated and out-of-equilibrium initial packages and ensembles of particles, as in Fig. 1. The initial Brownian-like growth of EB Eq. (34) is the black dashed line at short lag times. The EB_{st} plateaus for large x_0 given by Eq. (B12) are the red dashed horizontal lines. The terminal values EB($\Delta \rightarrow T$) given by Eq. (B13) are as the short red dashed lines at $\Delta \rightarrow T$. The value EB = 2 is the short blue horizontal line in the right top corner. Parameters: $\lambda = 1$, $\sigma = 1$, $dt = 0.01$, $T = 10^3$, and $N = 10^3$.

regime of EB, a stationary plateau emerges for long trajectories, with the value Eq. (B8). Finally, in the end of the trajectory, EB starts to increase and at $\Delta \rightarrow T$ it rapidly drops to a value given by Eq. (B11).

For *strongly nonequilibrium* initial positions, as described by Eq. (B7), the plateaus and terminal values of EB can considerably exceed unity. This emphasizes the importance of *higher moments* in the analysis of particle spreading; see also Ref. [73]. Results of computer simulations of harmonically-confined particles for a heavy-tailed distribution of initial positions are presented in Fig. 7. For this analysis the Student- T distribution

$$T_\nu(x_0) = \frac{\Gamma[(\nu+1)/2]}{\sqrt{\nu\pi} \Gamma[\nu/2]} \times \left(1 + \frac{[x_0/\bar{x}_0]^2}{\nu}\right)^{-\frac{\nu+1}{2}} \quad (36)$$

was employed. In Eq. (36), the lengthscale for initial displacements is \bar{x}_0 and $\Gamma[x]$ is the Γ function. One feature of T_ν is the fact that when the number of degrees of freedom $\nu \rightarrow 4$ the ratio of the fourth moment,

$$\langle x_0^4 \rangle = \int_{-\infty}^{+\infty} x_0^4 T_\nu(x_0) dx_0, \quad (37)$$

to the squared second moment of T_ν (kurtosis),

$$K = \langle x_0^4 \rangle / \langle x_0^2 \rangle^2 = 3(\nu-2)/(\nu-4), \quad (38)$$

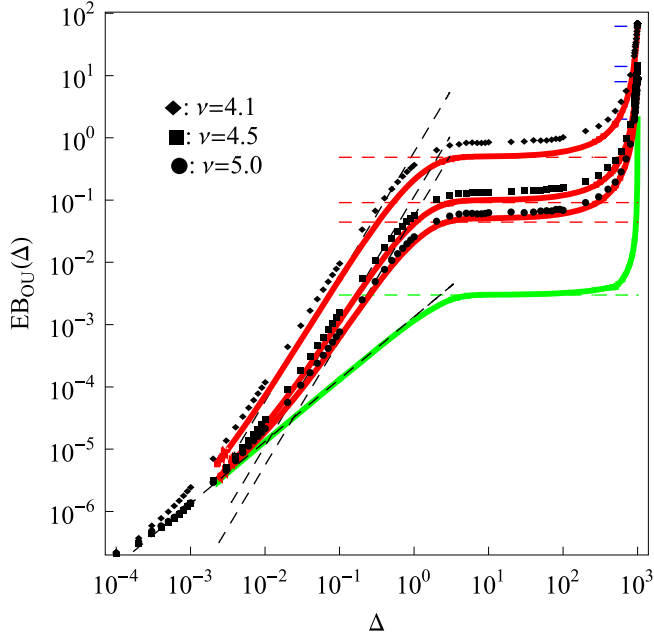


FIG. 7. EB_{OU} for initial positions from the Student- T distribution Eq. (36), as obtained from simulations. The green curve is the solution for equilibrium initial conditions, similar to Fig. 6, with respective asymptotes. The full analytical Eqs. (B4) and (B5) computed with the moments for $P(x_0) = T_\nu(x_0)$ are the red solid curves (nonequilibrium initial conditions). Approximate relations for the Brownian growth at short lag times Eq. (34) and the quadratic growth given by the second term in Eq. (B6) are the black dashed lines. The stationary plateau values Eq. (B8) are the red horizontal lines, for respective model parameters. The expansion Eq. (B11) near the terminal EB values is the short dashed black curves at $\Delta \rightarrow T$. The values of EB Eq. (B10) are the short blue dashed lines at $\Delta \rightarrow T$. Parameters are the same as in Fig. 6, except $\sigma = 100$, $\lambda = 1$. Averaging was performed over $N = 10^3$ initial positions for the selected ensemble of x_0 values yielding the kurtosis value closest to the analytical result Eq. (38).

as well as the excess kurtosis,

$$K_{ex} = K - 3 = 6/(\nu - 4), \quad (39)$$

diverge. Thus, at $\nu \rightarrow 4$ the higher-order moments contribute stronger to EB; see general Eqs. (B4) and (B5).

As a consequence, the evolution of $EB(\Delta)$ for long-tailed $P(x_0)$ differs dramatically from that observed for fixed particle starting positions, compare Figs. 7 and 6, respectively. In particular, in Fig. 7 we present the results for initial positions according to Eq. (36). We find a good agreement between theory and simulations in the entire range of lag times, for indices ν of the distribution $T_\nu(x_0)$ far from the critical value, see the curve for $\nu = 5$ in Fig. 7. As $\nu \rightarrow 4$ we encounter some deviations at intermediate lag times, as expected, see the curve for $\nu = 4.1$ in Fig. 7. As Fig. 7 illustrates, EB for $P(x_0)$ with $\langle x_0^4 \rangle \gg \langle x_0^2 \rangle^2$ is overall *much larger* than EB_{BM} (except for very short lag times and at $\Delta \rightarrow T$).

Note that considerably larger σ values were chosen in Fig. 7 to shift the region of the expected quadratic regime of $EB(\Delta)$ growth toward longer lag times. This, in turn, allowed us to keep the number of simulations points manageable and still observe all characteristic EB regimes for $T = 10^3$, used for

most other results. The final ensemble of initial x_0 points used for averaging in simulations for Fig. 7 was chosen from 10^5 samples of $N = 10^3$ points generated from Eq. (36). The selection criterion for the best x_0 -set was the closest value of the excess kurtosis, Eq. (39).

C. Einstein relation: Ensemble- and time-averaged displacements

The concept of linear response relates the first-order moment of particle displacements in the presence of small constant forces f to the second moment in the absence of a force [47,65,94,95,132,133]:

$$\langle x(t) - x_0 \rangle_f = \frac{f \langle [x(t) - x_0]^2 \rangle_{f=0}}{2k_B T}. \quad (40)$$

This relation was checked for a number of anomalous diffusion processes in the past [65,67,76,77]. For the first moments of the ensemble- and time-averaged displacements in the presence of a force, we find

$$\langle x(\Delta) - x_0 \rangle_f = (f\mu/\lambda - \langle x_0 \rangle)(1 - e^{-\lambda\Delta}) \quad (41)$$

and

$$\begin{aligned} \langle \delta^1(\Delta) \rangle_f &= \frac{1}{T - \Delta} \int_0^{T-\Delta} \langle [x(t + \Delta) - x(t)]^1 \rangle dt \\ &= \left(\frac{f\mu}{\lambda} - \langle x_0 \rangle \right) (1 - e^{-\lambda\Delta}) \frac{1 - e^{-\lambda(T-\Delta)}}{\lambda(T - \Delta)}. \end{aligned} \quad (42)$$

The second moments of the ensemble and time averages without force follow from Eqs. (11) and (15), respectively. We thus find that for the OU particles Eq. (40) is valid for the ensemble-averaged displacements if the initial positions satisfy the conditions $\langle x_0 \rangle = 0$ and $\langle x_0^2 \rangle = \langle x_{eq}^2 \rangle$. In this case, using Eqs. (10) and (5), we get $\langle (x(\Delta) - x_0)^2 \rangle = \sigma^2 \lambda^{-1} (1 - e^{-\lambda\Delta})$. For the time-averaged moments, the linear response relation is *generally not valid* because the first moment Eq. (42) explicitly depends on T , whereas the second-order force-free moment Eq. (15) at the same conditions does not, $\langle \delta^2(\Delta) \rangle = \sigma^2 \lambda^{-1} (1 - e^{-\lambda\Delta})$. The Einstein relation of type Eq. (40) for the *time-averaged* moments only hold at $\Delta \rightarrow T$.

III. DISCUSSION AND CONCLUSIONS

Despite the fact that the OU process is omnipresent in physical models and has been studied exhaustively over almost a century, we revealed and quantified a number of interesting and novel features of this process. They can be crucial for the analysis, interpretation, and understanding of experiments and computer simulations of diffusion in harmonic and other confining potentials.

A. Summary of key results

First, we demonstrated that *nonequilibrium* initial conditions for the stationary OU process may give rise to large discrepancies of the ensemble- and time-averaged MSDs following their standard definitions, see Eqs. (11) and (15), even in quasistationary domain of lag times. In the simple case of *equilibrium* starting conditions, however, the ensemble- and time-averaged MSDs are identical over the entire range

of times. As expected, they start linearly and saturate at long times at the plateau σ^2/λ . For initially-equilibrated particles full equivalence of ensemble and time averages is found.

For *nonequilibrium* initial conditions, the positions x_0 can either be fixed for all the particles or distributed. In the first scenario, the value of x_0 —the off-center position with respect to the bottom of the well—controls the timescale after which both the ensemble- and time-averaged MSDs *can* acquire a region of quadratic growth. We found that the initial linear increase is identical for both of these observables, namely, $\approx \sigma^2\Delta$. The subsequent quadratic growth can, however, be very different. For sufficiently long traces and substantial trap stiffness—such that $\lambda T \gg 1$ —the MSD starts the ballistic regime earlier and reaches the plateau with the magnitude independent on the trace length T .

The time-averaged MSD approaches a smaller plateau, with the value that depends on the trajectory length. The saturation to the plateau for the ensemble- and time-averaged MSDs takes place at lag times $\Delta \sim 1/\lambda$. The quadratic regime and the dramatic discrepancies of the ensemble- and time-averaged MSDs prior to and in the plateau regime can extend for a prolonged period of time. Toward the very end of the trajectory, as $\Delta \rightarrow T$, the ensemble-averaged MSD stays constant, while the time-averaged MSD grows rapidly and reaches the MSD plateau value. For progressively longer trajectories, this growth of the time-averaged MSD is increasingly abrupt.

Second, we quantified the behavior of EB in the entire range of lag times and for all choices of initial conditions. This parameter quantifies the amplitude variation of individual time-averaged MSD realizations. For *equilibrium* starting conditions, EB first grows with the lag time as for free BM, $EB(\Delta) \approx 4\Delta/(3T)$. For lag times $\Delta \gtrsim 1/\lambda$ the EB parameter starts to reach a plateau with the stationary value $EB_{st} \approx 3/(\lambda T)$. The longer the trajectory, the longer is the time span over which this plateau is found. For $\Delta \gtrsim T/2$ the ergodicity breaking parameter starts a *fast growth* and reaches the terminal value $EB=2$ at $\Delta = T$. We mention here that for the OU process $EB_{OU}(\Delta)$ is always smaller than $EB_{BM}(\Delta)$, as one might expect intuitively.

For *nonequilibrium fixed* off-centered initial particle conditions, for small x_0 the behavior of EB is similar to that for equilibrium conditions. For large x_0 values, after an initial Brownian-like growth, $EB(\Delta)$ saturates at a plateau with the value much smaller than for equilibrium starting positions. Specifically, the plateau value scales as $\propto 1/\langle x_0^2 \rangle$. Toward the end of the trajectory, EB increases slightly, and ultimately rapidly drops to a constant value that has the same scaling with x_0 as the stationary EB plateau itself.

For *nonequilibrium distributed* initial positions, the behavior of $EB(\Delta)$ is more involved. Namely, for a long-tailed $P(x_0)$ after the initial Brownian-like regime, a region of *quadratic*

growth of EB emerges. After this regime, at intermediate lag times, a stationary EB plateau is found, while $EB \rightarrow \langle x_0^4 \rangle / \langle x_0^2 \rangle^2 - 1$ at $\Delta \rightarrow T$. Therefore, we demonstrated that for starting particle positions obeying a distribution $P(x_0)$ with $\langle x_0^4 \rangle \gg \langle x_0^2 \rangle^2$ both the stationary plateau value and terminal value $EB(\Delta = T)$ can be much greater than unity.

B. Relation to single-particle tracking experiments

We expect that our theoretical predictions can be tested in single-particle tracking experiments in optical traps, such as optical tweezers. In particular, the behavior of $EB(\Delta)$ for different initial tracer conditions can potentially be probed *in vitro* or even inside live cells. For these purposes, the width of the optical traps should be set large enough so particle motions are restricted minimally. This can be achieved via reducing the trap stiffness, that is $\sim 0.01 \dots 1$ pN/nm [22,103,121] (depending, i.e., on laser power (k is linearly growing [117]), laser wavelength, particle size, and bead refractive index [115,134]). For a larger range of weakly-confined but still trackable particles one can examine the behavior of the time-averaged MSD and EB in a broader lag-time domain. Thereby, one can study the distinct behaviors and scaling regimes for these observables for various particle starting conditions, both equilibrium and nonequilibrium (fixed and distributed).

The features of these results can then be compared to severely restricted, almost jiggling motions of the tracers in strong traps [102]. The question here is whether the overall features of motion of trapped particles will measurably change with the stiffness of optical traps, and whether weak-trapping regime is realizable. Finally, extending the current approach to unveil the time-averaged and ergodic properties of the *fractional* OU process may be an interesting and challenging problem for the future.

ACKNOWLEDGMENTS

We thank K. Berg-Sørensen, J.-H. Jeon, E. P. Petrov, and C. Selhuber-Unkel for scientific discussions and correspondence on single-particle trapping and tracking experiments in cells. We acknowledge insightful comments of both referees; in particular, we thank the anonymous reviewer for pointing out Ref. [41]. A.G.C. thanks Maxim Cherstvy for help with checking the equations. R.M. and A.V.C. acknowledge financial support by the Deutsche Forschungsgemeinschaft (DFG Grants No. ME 1535/6-1 and No. ME 1535/7-1). R.M. also acknowledges support within Alexander von Humboldt Polish Honorary Research Scholarship. S.T. acknowledges the Deutscher Akademischer Austauschdienst (DAAD) for his Ph.D. Scholarship (Program ID No. 57214224).

APPENDIX A: FOURTH MOMENT OF TIME-AVERAGED DISPLACEMENTS

Here, the derivations of Eqs. (27) and (28) in the main text for the EB parameter given by Eq. (26) are presented. For this, we compute the fourth moment of particle displacements,

$$\langle (\overline{\delta^2(\Delta, T)})^2 \rangle = \frac{1}{(T - \Delta)^2} \int_0^{T-\Delta} dt_1 \int_0^{T-\Delta} dt_2 \langle [x(t_1 + \Delta) - x(t_1)]^2 [x(t_2 + \Delta) - x(t_2)]^2 \rangle, \quad (\text{A1})$$

where the integrand is the sum of nine terms, viz.

$$\begin{aligned}
 & \langle [x(t_1 + \Delta) - x(t_1)]^2 [x(t_2 + \Delta) - x(t_2)]^2 \rangle \\
 &= \langle x^2(t_1 + \Delta)x^2(t_2 + \Delta) - 2x^2(t_1 + \Delta)x(t_2 + \Delta)x(t_2) + x^2(t_1 + \Delta)x^2(t_2) - 2x(t_1 + \Delta)x(t_1)x^2(t_2 + \Delta) \\
 &+ 4x(t_1 + \Delta)x(t_1)x(t_2 + \Delta)x(t_2) - 2x(t_1 + \Delta)x(t_1)x^2(t_2) + x^2(t_1)x^2(t_2 + \Delta) - 2x^2(t_1)x(t_2 + \Delta)x(t_2) + x^2(t_1)x^2(t_2) \rangle.
 \end{aligned} \tag{A2}$$

For equilibrium initial conditions of the particles, the ensemble averages in Eq. (A2) can be computed using the two-point correlation function in Eq. (17), yielding

$$\begin{aligned}
 \langle (\overline{\delta^2(\Delta)})^2 \rangle &= \frac{1}{(T - \Delta)^2} \left(\frac{\sigma^2}{2\lambda} \right)^2 \int_0^{T-\Delta} dt_1 \int_0^{T-\Delta} dt_2 [2(1 + 2e^{-2\lambda|t_1-t_2|}) + (1 + 2e^{-2\lambda|t_1+\Delta-t_2|}) \\
 &+ (1 + 2e^{-2\lambda|t_1-t_2-\Delta|}) - 4(e^{-\lambda\Delta} + 2e^{-\lambda|t_1-t_2|}e^{-\lambda|t_1+\Delta-t_2|}) - 4(e^{-\lambda\Delta} + 2e^{-\lambda|t_1-t_2|}e^{-\lambda|t_1-\Delta-t_2|}) \\
 &+ 4(e^{-2\lambda\Delta} + e^{-2\lambda|t_1-t_2|} + e^{-\lambda|t_1+\Delta-t_2|}e^{-\lambda|t_1-t_2-\Delta|})].
 \end{aligned} \tag{A3}$$

The evaluation of $\langle (\overline{\delta^2(\Delta)})^2 \rangle$ is then reduced to computing only four different integrals, separately in the lag-time regions $0 < \Delta < T/2$ and $T/2 < \Delta < T$, denoted below by the respective subscripts. The double integration of Eq. (A3) in the two domains gives, respectively,

$$\begin{aligned}
 \langle (\overline{\delta^2(\Delta, T)})^2 \rangle_{<} &= \frac{\sigma^4}{4\lambda^2} \left[4 \left(1 - \frac{1}{\lambda^2(T - \Delta)^2} \right) (1 - e^{-\lambda\Delta})^2 + \frac{8}{\lambda(T - \Delta)} + \frac{4(T - 2\Delta)}{\lambda(T - \Delta)^2} (1 + e^{-2\lambda\Delta}) \right. \\
 &\left. - \frac{8(2T - 3\Delta)}{\lambda(T - \Delta)^2} \left(1 + \lambda\Delta - \frac{\lambda\Delta}{2} e^{-\lambda\Delta} \right) e^{-\lambda\Delta} + \frac{e^{-2\lambda T}}{\lambda^2(T - \Delta)^2} (1 - 4e^{\lambda\Delta} + 6e^{2\lambda\Delta} - 4e^{3\lambda\Delta} + e^{4\lambda\Delta}) \right]
 \end{aligned} \tag{A4}$$

and

$$\langle (\overline{\delta^2(\Delta, T)})^2 \rangle_{>} = \frac{\sigma^4}{4\lambda^2} \left[4(1 - 4e^{-\lambda\Delta} + 2e^{-2\lambda\Delta}) + \frac{8(1 - e^{-\lambda\Delta})}{\lambda(T - \Delta)} - \frac{1 - e^{-2\lambda(T-\Delta)}}{\lambda^2(T - \Delta)^2} (4 - 4e^{-\lambda\Delta} + e^{-2\lambda\Delta} - e^{-2\lambda(2\Delta-T)}) \right]. \tag{A5}$$

We checked that both the EB parameter constructed from the fourth-order moments Eqs. (A4) and (A5), according to Eq. (26), as well as the EB derivative with respect to the lag time are continuous at $\Delta = T/2$.

APPENDIX B: EB PARAMETER FOR NONEQUILIBRIUM INITIAL CONDITIONS

For *nonequilibrium* initial particle conditions, the pair-correlation function of Eq. (12) is no longer a function of the difference of two time moments only, as in Eq. (17). The expression for the four-point correlator of positions in Eq. (6) is therefore more complicated, involving the fourth and second moments of the initial positions,

$$\begin{aligned}
 \langle x(t')x(t'')x(t''')x(t''''') \rangle &= e^{-\lambda(t'+t''+t'''+t''''')} \left[\langle x_0^4 \rangle - 6\langle x_0^2 \rangle \left(\frac{\sigma^2}{2\lambda} \right) + 3 \left(\frac{\sigma^2}{2\lambda} \right)^2 \right] + \left[\langle x_0^2 \rangle \left(\frac{\sigma^2}{2\lambda} \right) - \left(\frac{\sigma^2}{2\lambda} \right)^2 \right] \left(e^{-\lambda(t'+t'')} e^{-\lambda|t''''-t'''} \right. \\
 &+ e^{-\lambda(t'+t''')} e^{-\lambda|t''''-t''} + e^{-\lambda(t'+t''''')} e^{-\lambda|t''''-t''} + e^{-\lambda(t''+t''''')} e^{-\lambda|t''''-t''} + e^{-\lambda(t''+t''''')} e^{-\lambda|t''''-t''} \\
 &\left. + e^{-\lambda(t'''+t''''')} e^{-\lambda|t''''-t''} \right) + \left(\frac{\sigma^2}{2\lambda} \right)^2 \left(e^{-\lambda|t''-t'''} e^{-\lambda|t''''-t'''} + e^{-\lambda|t''-t'''} e^{-\lambda|t''''-t'''} + e^{-\lambda|t''-t''''} e^{-\lambda|t''''-t'''} \right).
 \end{aligned} \tag{B1}$$

For *equilibrium* normally distributed initial positions x_0 the four-point correlator can be obtained using the Isserlis-Wick theorem,

$$\begin{aligned}
 \langle x(t')x(t'')x(t''')x(t''''') \rangle_{\text{eq}} &= (\langle x(t')x(t'') \rangle \langle x(t''')x(t''''') \rangle) + \langle x(t')x(t''') \rangle \langle x(t'')x(t''''') \rangle + \langle x(t')x(t''''') \rangle \langle x(t'')x(t''') \rangle)_{\text{eq}} \\
 &= \left(\frac{\sigma^2}{2\lambda} \right)^2 \left(e^{-\lambda|t''-t'''} e^{-\lambda|t''''-t'''} + e^{-\lambda|t''-t'''} e^{-\lambda|t''''-t'''} + e^{-\lambda|t''-t''''} e^{-\lambda|t''''-t'''} \right),
 \end{aligned} \tag{B2}$$

as for a Gaussian process at equilibrium,

$$\langle x_0^4 \rangle_{\text{eq}} = 3\langle x_0^2 \rangle_{\text{eq}}^2 = 3[\sigma^2/(2\lambda)]^2. \tag{B3}$$

For nonequilibrium initial conditions and with four-point correlator Eq. (B1) the derivation of EB is much more cumbersome. The exact results for arbitrary starting conditions are (using Wolfram Mathematica)

$$\begin{aligned}
 \text{EB}_{\text{OU}, <}(\Delta, T) &= \{-1 + [4e^{2\lambda(4\Delta+T)}\sigma^4 + 16e^{7\lambda\Delta+2\lambda T}\sigma^2(\sigma^2(-2 + 2\lambda\Delta - \lambda T) + 2\lambda(1 - 2\lambda\Delta + \lambda T)\langle x_0^2 \rangle) \\
 &+ e^{2\lambda(\Delta+T)}(-6\sigma^4 + 24\lambda\sigma^2\langle x_0^2 \rangle - 8\lambda^2\langle x_0^4 \rangle)]\}
 \end{aligned}$$

$$\begin{aligned}
& + 4e^{3\lambda\Delta+4\lambda T} (\sigma^4(17 + 2\lambda(11\Delta + 8\Delta^2\lambda - T(5 + 4\lambda T))) + 4\lambda\sigma^2(-3 + \lambda\Delta - 3\lambda T)\langle x_0^2 \rangle - 4\lambda^2\langle x_0^4 \rangle) \\
& + 4e^{\lambda(\Delta+4T)} (\sigma^4(1 + 2\lambda(\Delta + T)) - 4\lambda\sigma^2(-1 + \lambda(\Delta + T))\langle x_0^2 \rangle - 4\lambda^2\langle x_0^4 \rangle) \\
& + e^{4\lambda\Delta} (3\sigma^4 - 12\lambda\sigma^2\langle x_0^2 \rangle + 4\lambda^2\langle x_0^4 \rangle) - 4e^{5\lambda\Delta} (3\sigma^4 - 12\lambda\sigma^2\langle x_0^2 \rangle + 4\lambda^2\langle x_0^4 \rangle) \\
& + 6e^{6\lambda\Delta} (3\sigma^4 - 12\lambda\sigma^2\langle x_0^2 \rangle + 4\lambda^2\langle x_0^4 \rangle) - 4e^{7\lambda\Delta} (3\sigma^4 - 12\lambda\sigma^2\langle x_0^2 \rangle + 4\lambda^2\langle x_0^4 \rangle) \\
& + e^{8\lambda\Delta} (3\sigma^4 - 12\lambda\sigma^2\langle x_0^2 \rangle + 4\lambda^2\langle x_0^4 \rangle) + e^{4\lambda T} (3\sigma^4 - 12\lambda\sigma^2\langle x_0^2 \rangle + 4\lambda^2\langle x_0^4 \rangle) \\
& + 8e^{5\lambda\Delta+2\lambda T} (\sigma^4(-5 + 17\lambda\Delta - 15\lambda T) + 2\lambda^2\sigma^2(-17\Delta + 15T)\langle x_0^2 \rangle + 4\lambda^2\langle x_0^4 \rangle) \\
& + 8e^{3\lambda\Delta+2\lambda T} (3\sigma^4(1 + \lambda\Delta - \lambda T) - 6\lambda\sigma^2(2 + \lambda\Delta - \lambda T)\langle x_0^2 \rangle + 4\lambda^2\langle x_0^4 \rangle) \\
& + e^{4\lambda(\Delta+T)} (\sigma^4(-29 + 8\lambda(2\Delta^2\lambda + T(5 + 2\lambda T)) - \Delta(7 + 4\lambda T))) + 4\lambda\sigma^2(5 - 4\lambda\Delta + 4\lambda T)\langle x_0^2 \rangle + 4\lambda^2\langle x_0^4 \rangle) \\
& - 2e^{2\lambda(3\Delta+T)} (\sigma^4(-33 + 52\lambda\Delta - 36\lambda T) + 4\lambda\sigma^2(9 - 26\lambda\Delta + 18\lambda T)\langle x_0^2 \rangle + 4\lambda^2\langle x_0^4 \rangle) \\
& - 8e^{2\lambda(2\Delta+T)} (\sigma^4(2 + 11\lambda(\Delta - T)) - 2\lambda\sigma^2(7 + 11\lambda(\Delta - T))\langle x_0^2 \rangle + 6\lambda^2\langle x_0^4 \rangle) \\
& + e^{2\lambda(\Delta+2T)} (-2\sigma^4(23 + 4\lambda(\Delta(5 + 4\lambda\Delta) + T - 2\lambda T^2)) + 8\lambda\sigma^2(3 + 2\lambda\Delta + 6\lambda T)\langle x_0^2 \rangle + 24\lambda^2\langle x_0^4 \rangle)] / \\
& [(-1 + e^{\lambda\Delta})^2((-e^{2\lambda\Delta} + e^{3\lambda\Delta} + e^{2\lambda T})(\sigma^2 - 2\lambda\langle x_0^2 \rangle) + e^{\lambda(\Delta+2T)}(\sigma^2(-1 - 4\lambda\Delta + 4\lambda T) + 2\lambda\langle x_0^2 \rangle))^2] \quad (\text{B4})
\end{aligned}$$

and

$$\begin{aligned}
\text{EB}_{\text{OU}, >}(\Delta, T) = & \{-1 + [4e^{6\lambda T}\sigma^4 + e^{2\lambda(\Delta+T)}(-6\sigma^4 + 24\lambda\sigma^2\langle x_0^2 \rangle - 8\lambda^2\langle x_0^4 \rangle) \\
& + e^{2\lambda(3\Delta+T)}(\sigma^4(26 + 40\lambda(T - \Delta)) + 8\lambda\sigma^2(-1 + 10\lambda(\Delta - T))\langle x_0^2 \rangle - 8\lambda^2\langle x_0^4 \rangle) \\
& + e^{4\lambda\Delta}(3\sigma^4 - 12\lambda\sigma^2\langle x_0^2 \rangle + 4\lambda^2\langle x_0^4 \rangle) - 4e^{5\lambda\Delta}(3\sigma^4 - 12\lambda\sigma^2\langle x_0^2 \rangle + 4\lambda^2\langle x_0^4 \rangle) \\
& + 6e^{6\lambda\Delta}(3\sigma^4 - 12\lambda\sigma^2\langle x_0^2 \rangle + 4\lambda^2\langle x_0^4 \rangle) - 4e^{7\lambda\Delta}(3\sigma^4 - 12\lambda\sigma^2\langle x_0^2 \rangle + 4\lambda^2\langle x_0^4 \rangle) \\
& + e^{8\lambda\Delta}(3\sigma^4 - 12\lambda\sigma^2\langle x_0^2 \rangle + 4\lambda^2\langle x_0^4 \rangle) + e^{4\lambda T}(3\sigma^4 - 12\lambda\sigma^2\langle x_0^2 \rangle + 4\lambda^2\langle x_0^4 \rangle) \\
& + 8e^{5\lambda\Delta+2\lambda T}(\sigma^4(-3 + 13\lambda(\Delta - T)) - 2\lambda\sigma^2(2 + 13\lambda(\Delta - T))\langle x_0^2 \rangle + 4\lambda^2\langle x_0^4 \rangle) \\
& - 4e^{\lambda(\Delta+4T)}(\sigma^4(3 + 6\lambda\Delta - 6\lambda T) - 12\lambda\sigma^2(1 + \lambda\Delta - \lambda T)\langle x_0^2 \rangle + 4\lambda^2\langle x_0^4 \rangle) \\
& + 8e^{3\lambda\Delta+2\lambda T}(3\sigma^4(1 + \lambda\Delta - \lambda T) - 6\lambda\sigma^2(2 + \lambda\Delta - \lambda T)\langle x_0^2 \rangle + 4\lambda^2\langle x_0^4 \rangle) \\
& + e^{4\lambda(\Delta+T)}(\sigma^4(-29 + 8\lambda(\Delta - T)(-3 + 2\lambda\Delta - 2\lambda T)) + 4\lambda\sigma^2(5 - 4\lambda\Delta + 4\lambda T)\langle x_0^2 \rangle + 4\lambda^2\langle x_0^4 \rangle) \\
& - 4e^{3\lambda\Delta+4\lambda T}(\sigma^4(-9 + 2\lambda(\Delta - T)(1 + 8\lambda\Delta - 8\lambda T)) + 4\lambda\sigma^2(1 - 5\lambda\Delta + 5\lambda T)\langle x_0^2 \rangle + 4\lambda^2\langle x_0^4 \rangle) \\
& - 8e^{2\lambda(2\Delta+T)}(\sigma^4(2 + 11\lambda(\Delta - T)) - 2\lambda\sigma^2(7 + 11\lambda(\Delta - T))\langle x_0^2 \rangle + 6\lambda^2\langle x_0^4 \rangle) \\
& + 2e^{2\lambda(\Delta+2T)}(\sigma^4(-3 + 4\lambda(\Delta - T)(7 + 4\lambda\Delta - 4\lambda T)) - 4\lambda\sigma^2(5 + 14\lambda(\Delta - T))\langle x_0^2 \rangle + 12\lambda^2\langle x_0^4 \rangle)] / \\
& [(-1 + e^{\lambda\Delta})^2((-e^{2\lambda\Delta} + e^{3\lambda\Delta} + e^{2\lambda T})(\sigma^2 - 2\lambda\langle x_0^2 \rangle) + e^{\lambda(\Delta+2T)}(\sigma^2(-1 - 4\lambda\Delta + 4\lambda T) + 2\lambda\langle x_0^2 \rangle))^2] \}. \quad (\text{B5})
\end{aligned}$$

Equations (B4) and (B5) correspond to the lag-time regions $0 < \Delta < T/2$ and $T/2 < \Delta < T$, respectively. Here, we also checked that at $\Delta = T/2$ the EB parameter and its derivative over the lag time are continuous. For normally-distributed initial x_0 positions, when condition (B3) is satisfied, the general expressions in Eqs. (B4) and (B5) yield Eqs. (27) and (28) in the main text.

We now consider some limiting cases of the general Eqs. (B4) and (B5). For short lag times ($\Delta \ll T$) and long enough trajectories ($\lambda T \gg 1$) the Taylor expansion of Eq. (B4) for distributed starting positions yields

$$\text{EB}_{\text{OU}, <}(\Delta) \approx \frac{4\Delta}{3T} + \frac{\Delta^2}{24T^2} \left[-4\lambda T - \frac{20\lambda\langle x_0^2 \rangle}{\sigma^2} + \frac{6\lambda^2}{\sigma^4} (\langle x_0^4 \rangle - \langle x_0^2 \rangle^2) \right]. \quad (\text{B6})$$

Therefore, the leading order of EB for short lag times is the same as for BM, as expected. At later lag times, for strongly nonequilibrium positions x_0 , that is when

$$\langle x_0^4 \rangle \gg \langle x_0^2 \rangle^2 \text{ and } \langle x_0^2 \rangle \gg \sigma^2/(2\lambda), \quad (\text{B7})$$

a *quadratic regime* of EB(Δ) may emerge due to the second term in Eq. (B6). This behavior is expected, e.g., for long-tailed distributions $P(x_0)$. The plateau value of the EB parameter can be found via expansion of Eq. (B4) for distributed x_0 and long

traces,

$$EB_{OU,st} \sim \frac{1}{[4\lambda T + 2\lambda\langle x_0^2 \rangle / \sigma^2]^2} [48\lambda T - (1 - 2\lambda\langle x_0^2 \rangle / \sigma^2)^2 + 24\lambda\langle x_0^2 \rangle / \sigma^2 + 4\lambda^2(\langle x_0^4 \rangle - \langle x_0^2 \rangle^2) / \sigma^4]. \quad (B8)$$

For *equilibrium* starting conditions given by Eq. (16), Eqs. (29) and (31) in the main text follow from general Eqs. (B6) and (B8), respectively, for long traces when

$$\lambda T \gg \frac{\langle x_0^2 \rangle}{\sigma^2 / (2\lambda)}, \quad (B9)$$

as expected.

For OU-particles with starting positions distributed *strongly out of equilibrium*—when conditions of Eq. (B7) are satisfied and $\lambda T \ll 1$ —the stationary plateau Eq. (B8) can be simplified to

$$EB_{OU,st} \sim \langle x_0^4 \rangle / \langle x_0^2 \rangle^2 - 1. \quad (B10)$$

It depends only on the ratio of the fourth and second moments of a chosen $P(x_0)$. In this limit, the stationary value of EB depends only weakly on T , in contrast to the equilibrium result of Eq. (31). Expansion of Eq. (B5) at $\Delta \rightarrow T$ —when conditions of Eq. (B7) are satisfied—yields

$$EB_{OU, >(\Delta)} \approx \left(\frac{\langle x_0^4 \rangle}{\langle x_0^2 \rangle^2} - 1 \right) - \frac{(T - \Delta)2\sigma^2\langle x_0^4 \rangle}{\langle x_0^2 \rangle^3}. \quad (B11)$$

For *equilibrium* starting conditions of Eq. (16) the general expressions of Eq. (B5) reduce at $\Delta \rightarrow T$ to Eq. (30), with $EB=2$ at $\Delta = T$, as it should. Note that the first term in Eq. (B11) also reduces to $EB = 2$ when initial positions are distributed at equilibrium.

For nonequilibrium but *fixed* starting positions, when $\langle x_0^4 \rangle = \langle x_0^2 \rangle^2$, the stationary EB plateau value follows for long traces $\lambda T \gg 1$ from Eq. (B4) at intermediate lag times (for which still $\lambda\Delta \gg 1$) as

$$EB_{OU,st} \sim 6\sigma^2 / (\lambda\langle x_0^2 \rangle). \quad (B12)$$

For fixed starting conditions the terminal EB value at $\Delta \rightarrow T$ follows from Eq. (B8) in the limit $\langle x_0^2 \rangle \gg \sigma^2 / (2\lambda)$ as

$$EB(\Delta = T) \approx 2\sigma^2 / (\lambda\langle x_0^2 \rangle). \quad (B13)$$

[1] G. E. Uhlenbeck and L. S. Ornstein, On the theory of the Brownian motion, *Phys. Rev.* **36**, 823 (1930).
 [2] S. Chandrasekhar, Stochastic problems in physics and astronomy, *Rev. Mod. Phys.* **15**, 1 (1943).
 [3] M. C. Wang and G. E. Uhlenbeck, On the theory of the Brownian motion II, *Rev. Mod. Phys.* **17**, 323 (1945).
 [4] E. Nelson, *Dynamical Theories of Brownian Motion* (Princeton University Press, Princeton, NJ, 2001).
 [5] R. Kubo, M. Toda, and N. Hashitsume, *Statistical Physics II. Nonequilibrium Statistical Mechanics* (Springer-Verlag, Berlin/Heidelberg, 1985).
 [6] N. G. van Kampen, *Stochastic Processes in Physics and Chemistry* (Elsevier, Amsterdam, 1992).
 [7] R. Zwanzig, *Nonequilibrium Statistical Mechanics* (Oxford University Press, New York, 2001).
 [8] M. Gitterman, *The Noisy Oscillator: The First Hundred Years, From Einstein Until Now* (World Scientific, Singapore, 2005).
 [9] R. Brown, A brief account of microscopical observations made in the months of June, July, and August 1827, on the particles contained in the pollen of plants; and on the general existence of active molecules in organic and inorganic bodies, *Philos. Mag.* **4**, 161 (1828).
 [10] A. Einstein, Über die von der molekularkinetischen Theorie der Wärme geforderte Bewegung von in ruhenden Flüssigkeiten suspendierten Teilchen, *Ann. Physik* **322**, 549 (1905).
 [11] M. von Smoluchowski, Zur kinetischen Theorie der Brownschen Molekularbewegung und der Suspensionen, *Ann. Phys.* **326**, 756 (1906).
 [12] P. Langevin, Sur la théorie du mouvement brownien, *C. R. Acad. Sci. Paris* **146**, 530 (1908).
 [13] E. M. Stein and J. C. Stein, Stock price distributions with stochastic volatility: An analytic approach, *Rev. Finan. Studies* **4**, 727 (1991).
 [14] O. E. Barndorff-Nielsen and N. Shephard, Non-Gaussian Ornstein-Uhlenbeck-based models and some of their uses in financial economics, *J. R. Stat. Soc. Ser. B* **63**, 167 (2001).
 [15] O. E. Barndorff-Nielsen and N. Shephard, Econometric analysis of realized volatility and its use in estimating stochastic volatility models, *J. R. Stat. Soc. Ser. B* **64**, 253 (2002).
 [16] O. E. Barndorff-Nielsen, Superposition of Ornstein-Uhlenbeck type processes, *Theor. Prob. Appl.* **45**, 175 (2001).
 [17] L. F. James, G. Müller, and Z. Zhang, Stochastic volatility models based on OU-Gamma time change: theory and estimation, *J. Business Econ. Stat.* **36**, 75 (2018).

- [18] P. Hänggi, P. Talkner, and M. Borkovec, Reaction-rate theory: Fifty years after Kramers, *Rev. Mod. Phys.* **62**, 251 (1990).
- [19] A. Ashkin, J. M. Dziedzic, and T. Yamane, Optical trapping and manipulation of single cells using infrared laser beams, *Nature* **330**, 769 (1987).
- [20] A. Ashkin, Optical trapping and manipulation of neutral particles using lasers, *Proc. Natl. Acad. Sci. USA* **94**, 4853 (1997).
- [21] K. C. Neuman and S. M. Block, Optical trapping, *Rev. Sci. Instr.* **75**, 2787 (2004).
- [22] K. C. Neuman and A. Nagy, Single-molecule force spectroscopy: Optical tweezers, magnetic tweezers and atomic force microscopy, *Nature Meth.* **5**, 491 (2008).
- [23] M. A. Butler and A. A. King, Phylogenetic comparative analysis: A modeling approach for adaptive evolution, *Am. Natur.* **164**, 683 (2004).
- [24] B. Lindner, J. Garcia-Ojalvo, A. Neiman, and L. Schimansky-Geier, Effects of noise in excitable systems, *Phys. Rep.* **392**, 321 (2004).
- [25] T. Verechtaguina, I. M. Sokolov, and L. Schimansky-Geier, First passage time densities in resonate-and-fire models, *Phys. Rev. E* **73**, 031108 (2006).
- [26] L. Gammaitoni, P. Hänggi, P. Jung, and F. Marchesoni, Stochastic resonance, *Rev. Mod. Phys.* **70**, 223 (1998).
- [27] B. Leblanc and C. Scaillet, Path-dependent options on yield in the affine term structure model, *Finance Stochast.* **2**, 349 (1998).
- [28] L. Alili, P. Patie, and J. L. Pedersen, Representations of the first hitting time density of an Ornstein-Uhlenbeck process, *Stochast. Models* **21**, 967 (2004).
- [29] C. Yi, On the first passage time distribution of an Ornstein-Uhlenbeck process, *Quant. Finance* **10**, 957 (2010).
- [30] D. S. Grebenkov, First exit times of harmonically trapped particles: A didactic review, *J. Phys. A* **48**, 013001 (2015).
- [31] H. A. Kramers, Brownian motion in a field of force and the diffusion model of chemical reactions, *Physica* **7**, 284 (1940).
- [32] L. I. McCann, M. Dykman, and B. Golding, Thermally activated transitions in a bistable three-dimensional optical trap, *Nature* **402**, 785 (1999).
- [33] G. Volpe and G. Volpe, Simulation of a Brownian particle in an optical trap, *Am. J. Phys.* **81**, 224 (2013).
- [34] O. Yu. Sliusarenko, V. Yu. Gonchar, A. V. Chechkin, I. M. Sokolov, and R. Metzler, Kramers-like escape driven by fractional Gaussian noise, *Phys. Rev. E* **81**, 041119 (2010).
- [35] J. Gajda and A. Wylomanska, Time-changed Ornstein-Uhlenbeck process, *J. Phys. A* **48**, 135004 (2015).
- [36] Y. Hu and D. Nualart, Parameter estimation for fractional Ornstein-Uhlenbeck processes, *Stat. Probab. Lett.* **80**, 1030 (2010).
- [37] K. Tanaka, Maximum likelihood estimation for the nonergodic fractional Ornstein-Uhlenbeck process, *Stat. Inference Stoch. Process* **18**, 315 (2015).
- [38] P. Carr, H. Geman, D. B. Madan, and M. Yor, Stochastic volatility for Lévy processes, *Math. Finance* **13**, 345 (2003).
- [39] R. Toenjes, I. M. Sokolov, and E. B. Postnikov, Nonspectral Relaxation in One Dimensional Ornstein-Uhlenbeck Processes, *Phys. Rev. Lett.* **110**, 150602 (2013).
- [40] D. Janakiraman and K. L. Sebastian, Unusual eigenvalue spectrum and relaxation in the Lévy-Ornstein-Uhlenbeck process, *Phys. Rev. E* **90**, 040101(R) (2014).
- [41] D. S. Grebenkov, Time-averaged quadratic functionals of a Gaussian process, *Phys. Rev. E* **83**, 061117 (2011).
- [42] G. S. Agarwal, Brownian motion of a quantum oscillator, *Phys. Rev. A* **4**, 739 (1971).
- [43] F. Debbasch, K. Mallick, and J. P. Rivet, Relativistic Ornstein-Uhlenbeck process, *J. Stat. Phys.* **88**, 945 (1997).
- [44] B. U. Felderhof, Momentum relaxation of a relativistic Brownian particle, *Phys. Rev. E* **86**, 061103 (2012).
- [45] J. Dunkel and P. Hänggi, Theory of relativistic Brownian motion: The (1+3)-dimensional case, *Phys. Rev. E* **72**, 036106 (2005).
- [46] S. Jespersen, R. Metzler, and H. C. Fogedby, Lévy flights in external force fields: Langevin and fractional Fokker-Planck equations and their solutions, *Phys. Rev. E* **59**, 2736 (1999).
- [47] R. Metzler and J. Klafter, The random walk's guide to anomalous diffusion: A fractional dynamics approach, *Phys. Rep.* **339**, 1 (2000).
- [48] T. Kaarakka, Fractional Ornstein-Uhlenbeck processes, Ph.D. thesis, Tampere University of Technology, 2015.
- [49] S. Burov and M. Gitterman, Noisy oscillator: Random mass and random damping, *Phys. Rev. E* **94**, 052144 (2016).
- [50] R. C. Bourret, U. Frisch, and A. Pouquet, Brownian motion of harmonic oscillator with stochastic frequency, *Physica* **65**, 303 (1973).
- [51] C. B. Eab and S. C. Lim, Ornstein-Uhlenbeck process with fluctuating damping, *Physica A* **492**, 790 (2018).
- [52] M. V. Chubynsky and G. W. Slater, Diffusing Diffusivity: A Model for Anomalous, Yet Brownian, Diffusion, *Phys. Rev. Lett.* **113**, 098302 (2014).
- [53] A. G. Cherstvy and R. Metzler, Anomalous diffusion in time-fluctuating non-stationary diffusivity landscapes, *Phys. Chem. Chem. Phys.* **18**, 23840 (2016).
- [54] A. V. Chechkin, F. Seno, R. Metzler, and I. M. Sokolov, Brownian Yet Non-Gaussian Diffusion: From Superstatistics To Subordination of Diffusing Diffusivities, *Phys. Rev. X* **7**, 021002 (2017).
- [55] E. Yamamoto, T. Akimoto, A. C. Kalli, K. Yasuoka, and M. S. P. Sansom, Dynamic interactions between a membrane binding protein and lipids induce fluctuating diffusivity, *Science Adv.* **3**, e1601871 (2017).
- [56] J. Luczka, P. Talkner, and P. Hänggi, Diffusion of Brownian particles governed by fluctuating friction, *Physica A* **278**, 18 (2000).
- [57] J. C. Cox and S. A. Ross, The valuation of options for alternative stochastic processes, *J. Fin. Econ.* **3**, 145 (1976).
- [58] J. C. Cox, J. E. Ingersoll, and S. A. Ross, A theory of the term structure of interest rates, *Econometrica* **53**, 385 (1985).
- [59] L. O. Scott, Option pricing when the variance changes randomly: Theory, estimation, and an application, *J. Financ. Quant. Anal.* **22**, 419 (1987).
- [60] S. L. Heston, A closed-form solution for options with stochastic volatility with applications to bond and currency options, *Rev. Financ. Stud.* **6**, 327 (1993).
- [61] K. Hu, P. C. Ivanov, Z. Chen, P. Carpena, and H. E. Stanley, Effect of trends on detrended fluctuation analysis, *Phys. Rev. E* **64**, 011114 (2001).

- [62] F. Black and M. Scholes, The pricing of options and corporate liabilities, *J. Polit. Econ.* **81**, 637 (1973).
- [63] R. C. Merton, Option pricing when underlying stock returns are discontinuous, *J. Fin. Econ.* **3**, 125 (1976).
- [64] J.-P. Fouque, G. Papanicolaou, and K. R. Sircar, *Derivatives in Financial Markets with Stochastic Volatility* (Cambridge University Press, Cambridge, 2000).
- [65] Y. He, S. Burov, R. Metzler, and E. Barkai, Random Timescale Invariant Diffusion and Transport Coefficients, *Phys. Rev. Lett.* **101**, 058101 (2008).
- [66] S. Burov, J.-H. Jeon, R. Metzler, and E. Barkai, Single particle tracking in systems showing anomalous diffusion: The role of weak ergodicity breaking, *Phys. Chem. Chem. Phys.* **13**, 1800 (2011).
- [67] R. Metzler, J.-H. Jeon, A. G. Cherstvy, and E. Barkai, Anomalous diffusion models and their properties: non-stationarity, non-ergodicity, and ageing at the centenary of single particle tracking, *Phys. Chem. Chem. Phys.* **16**, 24128 (2014).
- [68] W. Deng and E. Barkai, Ergodic properties of fractional Brownian-Langevin motion, *Phys. Rev. E* **79**, 011112 (2009).
- [69] A. Andreanov and D. S. Grebenkov, Time-averaged MSD of Brownian Motion, *J. Stat. Mech.* (2012) P07001.
- [70] D. S. Grebenkov, Optimal and suboptimal quadratic forms for noncentered Gaussian processes, *Phys. Rev. E* **88**, 032140 (2013).
- [71] J.-H. Jeon and R. Metzler, Fractional Brownian motion and motion governed by the fractional Langevin equation in confined geometries, *Phys. Rev. E* **81**, 021103 (2010).
- [72] J.-H. Jeon and R. Metzler, Inequivalence of time and ensemble averages in ergodic systems: Exponential versus power-law relaxation in confinement, *Phys. Rev. E* **85**, 021147 (2012).
- [73] M. Schwarzl, A. Godec, and R. Metzler, Quantifying non-ergodicity of anomalous diffusion with higher order moments, *Sci. Rep.* **7**, 3878 (2017).
- [74] T. Neusius, I. M. Sokolov, and J. C. Smith, Subdiffusion in time-averaged, confined random walks, *Phys. Rev. E* **80**, 011109 (2009).
- [75] J. H. P. Schulz, E. Barkai, and R. Metzler, Aging Renewal Theory and Application to Random Walks, *Phys. Rev. X* **4**, 011028 (2014).
- [76] R. Hou, A. G. Cherstvy, R. Metzler, and T. Akimoto, Biased continuous-time random walks for ordinary and equilibrium cases: Facilitation of diffusion, ergodicity breaking and ageing, *Phys. Chem. Chem. Phys.* **20**, 20827 (2018).
- [77] T. Akimoto, A. G. Cherstvy, and R. Metzler, Enhancement, slow relaxation, ergodicity and rejuvenation of diffusion in biased continuous-time random walks, *Phys. Rev. E* **98**, 022105 (2018).
- [78] A. G. Cherstvy, A. V. Chechkin and R. Metzler, Anomalous diffusion and ergodicity breaking in heterogeneous diffusion processes, *New J. Phys.* **15**, 083039 (2013).
- [79] A. G. Cherstvy and R. Metzler, Nonergodicity, fluctuations, and criticality in heterogeneous diffusion processes, *Phys. Rev. E* **90**, 012134 (2014).
- [80] A. G. Cherstvy, A. V. Chechkin, and R. Metzler, Ageing and confinement in non-ergodic heterogeneous diffusion processes, *J. Phys. A* **47**, 485002 (2014).
- [81] A. G. Cherstvy and R. Metzler, Ergodicity breaking, ageing, and confinement in generalized diffusion processes with position and time dependent diffusivity, *J. Stat. Mech.* (2015) P05010.
- [82] H. Safdari, A. V. Chechkin, G. R. Jafari, and R. Metzler, Aging scaled Brownian motion, *Phys. Rev. E* **91**, 042107 (2015).
- [83] A. Bodrova, A. V. Chechkin, A. G. Cherstvy, and R. Metzler, Ultraslow scaled Brownian motion, *New J. Phys.* **17**, 063038 (2015).
- [84] H. Safdari, A. G. Cherstvy, A. V. Chechkin, F. Thiel, I. M. Sokolov, and R. Metzler, Quantifying the nonergodicity of scaled Brownian motion, *J. Phys. A* **48**, 375002 (2015).
- [85] A. Bodrova, A. V. Chechkin, A. G. Cherstvy, H. Safdari, I. M. Sokolov, and R. Metzler, Underdamped scaled Brownian motion: (Non)existence of the overdamped limit in anomalous diffusion, *Sci. Rep.* **6**, 30520 (2016).
- [86] I. Goychuk and V. O. Kharchenko, Anomalous Features of Diffusion in Corrugated Potentials with Spatial Correlations: Faster Than Normal, and Other Surprises, *Phys. Rev. Lett.* **113**, 100601 (2014).
- [87] W. Guo, Y. Li, W.-H. Song, and L.-C. Du, Ergodicity breaking and aging of underdamped Brownian dynamics with quenched disorder, *J. Stat. Mech.* (2018) 033303.
- [88] A. A. Budini, Memory-induced diffusive-superdiffusive transition: Ensemble and time-averaged observables, *Phys. Rev. E* **95**, 052110 (2017).
- [89] A. Godec and R. Metzler, Finite-Time Effects and Ultraweak Ergodicity Breaking in Superdiffusive Dynamics, *Phys. Rev. Lett.* **110**, 020603 (2013).
- [90] E. Barkai, Y. Garini, and R. Metzler, Strange kinetics of single molecules in living cells, *Phys. Today* **65**(8), 29 (2012).
- [91] J.-P. Bouchaud, Weak ergodicity breaking and aging in disordered systems, *J. Phys. I France* **2**, 1705 (1992).
- [92] G. Bel and E. Barkai, Weak Ergodicity Breaking in the Continuous-Time Random Walk, *Phys. Rev. Lett.* **94**, 240602 (2005).
- [93] A. Rebenshtok and E. Barkai, Distribution of Time-Averaged Observables for Weak Ergodicity Breaking, *Phys. Rev. Lett.* **99**, 210601 (2007).
- [94] J.-P. Bouchaud and A. Georges, Anomalous diffusion in disordered media: Statistical mechanisms, models and physical applications, *Phys. Rep.* **195**, 127 (1990).
- [95] R. Metzler and J. Klafter, The restaurant at the end of the random walk: Recent developments in the description of anomalous transport by fractional dynamics, *J. Phys. A* **37**, R161 (2004).
- [96] I. M. Sokolov, Models of anomalous diffusion in crowded environments, *Soft Matter* **8**, 9043 (2012).
- [97] F. Höfling and T. Franosch, Anomalous transport in the crowded world of biological cells, *Rep. Prog. Phys.* **76**, 046602 (2013).
- [98] Y. Meroz and I. M. Sokolov, A toolbox for determining subdiffusive mechanisms, *Phys. Rep.* **573**, 1 (2015).
- [99] J.-H. Jeon, N. Leijnse, L. B. Oddershede, and R. Metzler, Anomalous diffusion and power-law relaxation of the time-averaged mean-squared displacement in wormlike micellar solutions, *New J. Phys.* **15**, 045011 (2013).
- [100] I. M. Tolic-Nørrelykke, E.-L. Munteanu, G. Thon, L. Oddershede, and K. Berg-Sørensen, Anomalous Diffusion in Living Yeast Cells, *Phys. Rev. Lett.* **93**, 078102 (2004).
- [101] I. Golding and E. C. Cox, Physical Nature of Bacterial Cytoplasm, *Phys. Rev. Lett.* **96**, 098102 (2006).

- [102] J.-H. Jeon, V. Tejedor, S. Burov, E. Barkai, C. Selhuber-Unkel, K. Berg-Sørensen, L. Oddershede, and R. Metzler, *In vivo* Anomalous Diffusion and Weak Ergodicity Breaking of Lipid Granules, *Phys. Rev. Lett.* **106**, 048103 (2011).
- [103] L. B. Oddershede, Force probing of individual molecules inside the living cell is now a reality, *Nature Chem. Biol.* **8**, 879 (2012).
- [104] E. Bertseva, D. S. Grebenkov, P. Schmidhauser, S. Gribkova, S. Jeney, and L. Forro, Optical trapping microrheology in cultured human cells, *Eur. Phys. J. E* **35**, 63 (2012).
- [105] N. Gal, D. Lechtman-Goldstein, and D. Weihs, Particle tracking in living cells: a review of the mean square displacement method and beyond, *Rheol. Acta* **52**, 425 (2013).
- [106] D. S. Grebenkov, M. Vahabi, E. Bertseva, L. Forro, and S. Jeney, Hydrodynamic and subdiffusive motion of tracers in a viscoelastic medium, *Phys. Rev. E* **88**, 040701(R) (2013).
- [107] S. C. Weber, A. J. Spakowitz, and J. A. Theriot, Bacterial Chromosomal Loci Move Subdiffusively Through a Viscoelastic Cytoplasm, *Phys. Rev. Lett.* **104**, 238102 (2010).
- [108] S. M. A. Tabei, S. Burov, H. Y. Kim, A. Kuznetsov, T. Huynh, J. Jureller, L. H. Philipson, A. R. Dinner, and N. F. Scherer, Intracellular transport of insulin granules is a subordinated random walk, *Proc. Natl. Acad. Sci. USA* **110**, 4911 (2013).
- [109] O. M. Marago, P. H. Jones, P. G. Gucciardi, G. Volpe, and A. C. Ferrari, Optical trapping and manipulation of nanostructures, *Nature Nanotech.* **8**, 807 (2013).
- [110] K. Nørregaard, R. Metzler, C. Ritter, K. Berg-Sørensen, and L. Oddershede, Manipulation and motion of organelles and single molecules in living cells, *Chem. Rev.* **117**, 4342 (2017).
- [111] H. Shen, L. J. Tausin, R. Baiyasi, W. Wang, N. Moringo, B. Shuan, and C. F. Landes, Single particle tracking: From theory to biophysical applications, *Chem. Rev.* **117**, 7331 (2017).
- [112] M. J. Saxton and K. Jacobson, Single-particle tracking: Applications to membrane dynamics, *Annu. Rev. Biophys. Biomol. Struct.* **26**, 373 (1997).
- [113] K. Svoboda and S. M. Block, Biological applications of optical forces, *Annu. Rev. Biophys. Biomol. Struct.* **23**, 247 (1994).
- [114] R. W. Bowman and M. J. Padgett, Optical trapping and binding, *Rep. Prog. Phys.* **76**, 026401 (2013).
- [115] J. Mas, A. C. Richardson, S. N. S. Reihani, L. B. Oddershede, and K. Berg-Sørensen, Quantitative determination of optical trapping strength and viscoelastic moduli inside living cells, *Phys. Biol.* **10**, 046006 (2013).
- [116] M. Fischer, A. C. Richardson, S. N. S. Reihani, L. B. Oddershede, and K. Berg-Sørensen, Active-passive calibration of optical tweezers in viscoelastic media, *Rev. Sci. Instr.* **81**, 015103 (2010).
- [117] S. Bera, S. Paul, R. Singh, D. Ghosh, A. Kundu, A. Banerjee, and R. Adhikari, Fast Bayesian inference of optical trap stiffness and particle diffusion, *Sci Rep.* **7**, 41638 (2017).
- [118] S. F. Tolic-Nørrelykke, E. Schäffer, J. Howard, F. S. Pavone, F. Jülicher, and H. Flyvbjerg, Calibration of optical tweezers with positional detection in the back focal plane, *Rev. Sci. Instr.* **77**, 103101 (2006).
- [119] M. Fischer and K. Berg-Sørensen, Calibration of trapping force and response function of optical tweezers in viscoelastic media, *J. Optics A* **9**, S239 (2007).
- [120] A. Rohrbach, Stiffness of Optical Traps: Quantitative Agreement Between Experiment and Electromagnetic Theory, *Phys. Rev. Lett.* **95**, 168102 (2005).
- [121] D. Y. Lee, C. Kwon, and H. K. Pak, Nonequilibrium Fluctuations for a Single-Particle Analog of Gas in a Soft Wall, *Phys. Rev. Lett.* **114**, 060603 (2015).
- [122] M. Lindner, G. Nir, A. Vivante, I. T. Young, and Y. Garini, Dynamic analysis of a diffusing particle in a trapping potential, *Phys. Rev. E* **87**, 022716 (2013).
- [123] S. B. Smith, L. Finzi, and C. Bustamante, Direct mechanical measurements of the elasticity of single DNA molecules by using magnetic beads, *Science* **258**, 1122 (1992).
- [124] V. Tejedor, O. Benichou, R. Voituriez, R. Jungmann, F. Simmel, C. Selhuber-Unkel, L. B. Oddershede, and R. Metzler, Quantitative analysis of single particle trajectories: Mean maximal excursion method, *Biophys. J.* **98**, 1364 (2010).
- [125] M. Magdziarz, A. Weron, K. Burnecki, and J. Klafter, Fractional Brownian Motion Versus the Continuous-Time Random Walk: A Simple Test for Subdiffusive Dynamics, *Phys. Rev. Lett.* **103**, 180602 (2009).
- [126] E. Kepten, A. Weron, G. Sikora, R. Burnecki, and Y. Garini, Guidelines for the fitting of anomalous diffusion mean square displacement graphs from single particle tracking experiments, *PLoS ONE* **10**, e0117722 (2015).
- [127] V. Briane, C. Kervrann, and M. Vimondz, A statistical analysis of particle trajectories in living cells, *Phys. Rev. E* **97**, 062121 (2018).
- [128] T. Wagner, A. Kroll, C. R. Haramagatti, H.-G. Lipinski, and M. Wiemann, Classification and segmentation of nanoparticle diffusion trajectories in cellular micro environments, *PLoS ONE* **12**, e0170165 (2017).
- [129] C. C. Fritsch and J. Langowski, Kinetic lattice Monte Carlo simulation of viscoelastic subdiffusion, *J. Chem. Phys.* **137**, 064114 (2012).
- [130] S. M. Rytov, Yu. A. Kravtsov, and V. I. Tatarskii, *Principles of Statistical Radiophysics I: Elements of Random Process Theory* (Springer, Heidelberg, 1987).
- [131] D. S. Grebenkov, Probability distribution of the time-averaged mean-square displacement of a Gaussian process, *Phys. Rev. E* **84**, 031124 (2011).
- [132] E. Barkai and Y.-C. Cheng, Aging continuous-time random walks, *J. Chem. Phys.* **118**, 6167 (2003).
- [133] V. Blickle, T. Speck, C. Lutz, U. Seifert, and C. Bechinger, Einstein Relation Generalized to Nonequilibrium, *Phys. Rev. Lett.* **98**, 210601 (2007).
- [134] F. Catala, F. Marsa, M. Montes-Usategui, A. Farre, and E. Martin-Badosa, Extending calibration-free force measurements to optically trapped rod-shaped samples, *Sci. Rep.* **7**, 42960 (2017).